

THESIS



This is to certify that the

thesis entitled

## STRUCTURE AND FUNCTIONAL DOMAINS IN PHOSPHOLAMBAN: RELATIONSHIP TO BIOLOGICAL ACTIVITY IN CARDIAC SARCOPLASMIC RETICULUM

presented by

Helena Xiaoying Ouyang

has been accepted towards fulfillment of the requirements for

M.S. degree in Food Science

Major professor ~

Date (1) 5, 1993

**O**-7639

MSU is an Affirmative Action/Equal Opportunity Institution

### LIBRARY Michigan State University

PLACE IN RETURN BOX to remove this checkout from your record.

TO AVOID FINES return on or before date due.

DATE DUE	DATE DUE	DATE DUE
TAN I I WAR		
	<u>.</u>	

MSU Is An Affirmative Action/Equal Opportunity Institution
characteristics.pm3-p.1

# STRUCTURE AND FUNCTIONAL DOMAINS IN PHOSPHOLAMBAN: RELATIONSHIP TO BIOLOGICAL ACTIVITY IN CARDIAC SARCOPLASMIC RETICULUM

BY

Helena Xiaoying Ouyang

#### A THESIS

Submitted to
Michigan State University
in partial fulfillment of the requirements
for the degree of

MASTER OF SCIENCE

Department of Food Science and Human Nutrition

1993

#### ABSTRACT

#### STRUCTURE AND FUNCTIONAL DOMAINS IN PHOSPHOLAMBAN: RELATIONSHIP TO BIOLOGICAL ACTIVITY IN CARDIAC SARCOPLASMIC RETICULUM

By

#### Helena Xiaoying Ouyang

A synthetic peptide corresponding to the cytoplasmic portion of phospholamban (PLB) residues 1-25 was utilized for defining calmodulin (CaM) binding domain and the affinity of the binding. Threedythedasmic region of PLB is form an amphiphilic  $\alpha$ -helix. The fluorescent studies showed that PLB and CaM form a 1:1 complex by binding the C domain of CaM with a dissociation constant (K<sub>4</sub>) of 7  $\mu$ M. Phosphorylation PLB decreased its affinity to the CaM (K=16.78). Increasing ionic strength resulted in breaking up CaM-PLB complex, which suggests that the electrostatic forces rather than hydrophobic forces play an important role in stabilizing the CaM-PLB complex. The first 6 residues of PLB peptide were removed by  $\alpha$ -chymotrypsin for studying the interacting portion of PLB with CaM. Residues 7-25 of the peptide were not phosphorylated by CaM-dependent protein kinase, but were phosphorylated by cAMP-dependent protein kinase. The results indicate that the first 6 residues of PLB constitute the domain for CaM binding, and suggest that the formation of a PLB-CaM complex is a key step for activating CaM-protein kinase.

This is dedicated to my parents

#### **ACKNOWLEDGMENTS**

First and foremost, I would like to express my sincere thanks to my thesis advisor, Dr. Gale M. Strasburg. His guidance, support and encouragement are absolutely crucial for the finish of this thesis. His deep understanding of food science problems, both experimental and theoretical; his attitude about doing food science, paying attention to every details, have a profound influence on my career. Special thanks go to Dr. A. Haug for being on my graduate committee and for reviewing my thesis in such a short time notice.

I want to express my gratitude to members of my graduate committee, Dr. W.G. Helferich and Dr. R.A. Merkel. Their generous advice and suggestions on the thesis are appreciated.

No acknowledgement would be complete without mentioning the help received from people who have helped and collaborated on my thesis. I would like to thank my laboratory technician Mark Reedy and my fellow graduate student Hsiu Ching Yang for their help and patience. I appreciate Sabine Helling for correcting my English problems.

Finally, I would like to express my deepest gratitude to my parents, brothers and my husband, Qiubao Pan for their continual love and support of my study. I wish to thank Qiubao's patience, understanding and interesting in my studying area. I hope to give my deep thanks to my uncles, Keliang and Keyou Ouyang.

#### TABLE OF CONTENTS

	Page
LIST OF FIGURES	vi
LITERATURE REVIEW (Introduction)	1
INTRODUCTION TO FLUORESCENCE SPECTROSCOPY	16
MATERIALS AND METHODS	29
RESULTS AND DISCUSSION	39
CONCLUSION	74
LITERATURE CITED	75

#### LIST OF FIGURES

		Page
Figure 1	1.	Schematic representation of mammalian cardiac sarcoplasmic reticulum and T-tubules (From Fawcett and McNutt, 1969, J. Cell Biol. 42,24
Figure 2	2.	Reaction scheme of Ca-ATPase. E and E~P represent non-phosphorylated and phosphorylated Ca-ATPase, respectively. 1 and 2 indicate inside and outside of the SR membrane (From de Meis and Vianna, 1979, Ann. Rev. Biochem. 48, 280)6
Figure 3	3.	Helical wheel diagram of phospholamban residues 2-16. It is characterized as an amphiphilic, α-helical portion of PLB. The hydrophobic cluster consists of Val 4, Thr 8, Ile 12 and Ala 15 (From Gao, Levine, Mornet, Slatter and Strasburg, 1993, Biochim. Biophys. Acta, 1160, 29)13
Figure 4	4.	Schematic energy-level diagram (From Lakowicz, Principles of Fluorescence Spectroscopy, 4)17
Figure 5	5.	Schematic diagram of the components of a spectrofluorometer (From Lakowicz, Principles of Fluorescence Spectroscopy, 21)
Figure 6	6.	Cross-sectional diagram of a diffraction grating (From Guilbault, Practical Fluorescence, 48)21
Figure 7		Titration of 1 $\mu$ M rhodamine-X-maleimide labeled wheat germ CaM with PLB peptide (20 mM PIPES, pH 7.5 and 0.1 mM CaCl <sub>2</sub> ; excitation wavelength: 580 nm, emission wavelength: 605 nm)41
Figure 8	В.	Titration of 1 $\mu$ M rhodamine-X-maleimide labeled site-specific mutant chicken CaM (Q143C CaM) with PLB peptide (20 mM PIPES, pH 7.0, 0.1 M NaCl and 0.1 mM CaCl <sub>2</sub> ; excitation wavelength: 580 nm, emission wavelength: 605 nm
Figure 9	9.	Scatchard plot of rhodamine-X-maleimide-labeled Q143C CaM titration. The value of the dissociation constant ( $K_d$ ) and the maximum binding capacity ( $B_{max}$ ) are 1.64 $\mu$ M and 1.083 x $10^{-3}$ $\mu$ M, respectively
Figure 1	10.	Fluorescence anisotropy measurement upon

	titration of rhodamine-X-maleimide labeled Q143C CaM with the PLB peptide45
Figure	11. Fluorescence anisotropy change of rhodamine-X-maleimide-labeled Q143C CaM vs concentration of PLB peptide. Kd=2.69 $\mu$ M46
Figure	12. Molecular structures of rhodamine-X-maleimide and N-((2(iodoacetoxy)ethyl-N-methyl)-amino-7-nitrobenz-2-oxa-1,3 -diazole) (IANBD)47
Figure	13. Fluorescence emission scan of IANBD-labeled Q1430 CaM in the presence and absence of the PLB peptide. The excitation wavelength was 475 nm. (20 mM PIPES, pH 7.0, 0.1 M NaCl and 0.1 mM CaCl <sub>2</sub> )
Figure	14. Fluorescence change upon titration of IANBD-labeled Q143C CaM with PLB peptide in 20 mM PIPES, pH 7.0, 0.1 M NaCl and 0.1 mM CaCl <sub>2</sub> . The excitation wavelength was 475 nm; the emission wavelength was 537 nm
Figure	15. Fluorescence emission spectrum of IANBD-labeled Q143C CaM in the absence and presence of melittin. The excitation wavelength was 475 nm. (20 mM PIPES, pH 7.0, 0.1 M NaCl and 0.1 mM CaCl <sub>2</sub> )53
Figure	16. Titration of IANBD-labeled Q143C CaM with melittin. The beffer conditions were 20 mM PIPES, pH 7.0, 0.1 M NaCl and 0.1 mM CaCl <sub>2</sub> . The excitation wavelength was 475nm; the emission wavelength was 537 nm)
Figure	17. Scatchard plot of titration of IANBD-labeled Q143C CaM with PLB peptide. Kd=7 $\mu$ M, B <sub>max</sub> =0.98 $\mu$ M55
Figure	18. Titration of IANBD-labeled Q143C CaM with cAMP-dependent protein kinase phosphorylated PLB peptide. The buffer conditions were 20 mM PIPES, pH 7.0 and 0.1 mM CaCl <sub>2</sub> . The excitation wavelength was 475 nm; the emission wavelength was 537 nm)
Figure	19. Scatchard plot of titration of IANBD-labeled Q143C CaM with phosphorylated PLB peptide. Kd=16.78 $\mu$ M, B <sub>max</sub> =1 $\mu$ M
Figure	20. Helical wheel diagram of peptide LK2 (FMOC-(Leu-Lys-Lys-Leu-Lys-Leu) <sub>2</sub> and phospholamban residues 2-16 (From Cox, Comte, Fitton and

		DeGrado, 1985, J. Blol. Chem. 200, 2555)
Figure	21	Titration of IANBD-labeled Q143C CaM with KCl in the absence ( $\Delta$ ) or presence ( $\Delta$ ) of 30 $\mu$ M PLB peptide. The buffer condition were 20 mM PIPES, pH 7.0 and 0.1 mM CaCl <sub>2</sub> . The excitation wavelength was 475 nm; the emission wavelength was 537 nm)
Figure	22	Amino acid sequence of PLB. (From Fujii, Ueno, Kitano, Tanaka, Kadoma and Tada, 1987, J. Clin. Invest. 79, 301-304; Strasburg, Hanson, Ouyang and Louis, 1993, Biochim. Biophys. Acta, In press)
Figure	23	HPLC elution profile of α-chymotrypsin digested PLB peptide. The peptide eluting at 31 minutes was sequenced by Edman degradation and identified as residues 7-25 (From Strasburg, Hanson, Ouyang and Louis, 1993, Biochim. Biophys. Acta, In press)
Figure	24	Autoradiogram of phosphorylation of $\alpha$ -chymotrypsin digested PLB peptide by CaM-dependent protein kinase. 5 $\mu$ g of digested PLB peptide were phosphorylated in 20 mM HEPES, pH 6.8, 0.1 mM CaCl <sub>2</sub> , 10 mM MgCl <sub>2</sub> , 1 $\mu$ M wheat germ CaM, 1 mg/ml longitudinal SR vesicles and 0.1 mM AT <sup>32</sup> P. The gel was exposed for 24 hours. The concentrations of $\alpha$ -chymotrypsin are: Lane 1: 0 $\mu$ g/ml, Lane 2: 2 $\mu$ g/ml, Lane 3: 5 $\mu$ g/ml, Lane 4: 10 $\mu$ g/ml, Lane 5, 20 $\mu$ g/ml. Odd and even numbered lanes represent SR membrane and supernatants which contain phosphorylated PLB peptide, respectively68
Figure	25	Percentage of phosphorylations of chymotrypsin-digested PLB peptide as a function of chymotrypsin concentration70
Figure	26	Autoradiogram of phosphorylation of PLB peptide 1-25 and 7-25 by CaM- and cAMP-dependent protein kinase. Five μg of the peptides were phosphorylated in 20 mM HEPES, pH 6.8, 10 mM MgCl <sub>2</sub> , 2 mM EGTA, 10 mM cAMP, 0.25 mg/ml protein kinase and 0.1 mM AT <sup>32</sup> P for cAMP-dependent phosphorylation. For CaM-dependent phosphorylation, 5 μg of peptide were phosphorylated in 20 mM HEPES, pH 6.8, 0.1 mM CaCl <sub>2</sub> , 10 mM MgCl <sub>2</sub> , 1 μM wheat germ CaM, 1 mg/ml longitudinal SR vesicles and 0.1 mM AT <sup>32</sup> P. The peptides were separated from the SR membrane and resolved in a 20% polyacrylamide gel, and the gel was dried and was exposed for 24 hours. The

#### LITERATURE REVIEW

Muscle contraction is induced when calcium (Ca<sup>2+</sup>) ion is released from the sarcoplasmic reticulum (SR) into the muscle sarcoplasm upon depolarization of the cell. Ca<sup>2+</sup> binds to the troponin complex, which together with actin and tropomyosin, is located along the thin filament (Ebashi et al., 1968). The Ca<sup>2+</sup>-induced conformational change in troponin is transmitted to tropomyosin and actin, resulting in actomyosin crossbridge formation and force development. When the nerve signal ceases, Ca<sup>2+</sup> is pumped back into the SR, crossbridge formation is inhibited and the muscle relaxes.

A factor capable of inducing relaxation of myofibrillar bundles was first found in the 1950s in an aqueous extract of muscle (Marsh et al., 1951; Bendall, 1952, 1958). The relaxing activity was associated with the microsomal fraction of muscle which possessed a Mg<sup>2+</sup>-dependent ATPase activity and consisted of membrane vesicles (Kumagi et al., 1955; Ebashi, 1960; Nagai et al., 1960; Ebashi et al., 1962; Muscatello et al., 1961, 1962). Hasselbach et al. (1961) and Ebashi et al. (1961, 1962) demonstrated that a significant amount of Ca<sup>2+</sup> could be removed from the medium in the presence of ATP and Mg<sup>2+</sup> by the microsomal fraction. The ATPase activity of the microsomal vesicles was activated by the addition of Ca<sup>2+</sup> and Mg<sup>+</sup> (Hasselbach, 1961; 1963).

Porter (1961) and Muscatello et al. (1961, 1962) indicated that the microsomal vesicles possessing relaxing activity are derived from the sarcoplasmic reticulum. As shown by Figure 1 (Fawcett and McNutt, 1969), the SR consists of a membrane-limited reticular structure of continuous vesicles, tubules and cisternae which form a network surrounding the myofibril (Bennett et al., 1953; Franzini et al., 1975; Porter, 1957, 1961; Peachey, 1965, 1968). These workers showed that another tubular structure, the t-tubule, runs perpendicularly to the terminal cisterna, a part of the SR that is thickened to form a continuous sac. The membrane of the t-tubule system was found to be a continuation of the sarcolemma; thus, the t-tubule lumen is a continuation of the extracellular space (Endo, 1964; Franzini et al., 1975; Huxley, 1964).

Kamada et al. (1943) and Heilbrunn et al. (1947) first observed at the injection of Ca<sup>2+</sup> into a muscle fiber can induce local contraction. The latter authors also suggested that the contractile process in muscle in vivo is induced by Ca<sup>2+</sup>. Later several investigators demonstrated that a minute amount of Ca<sup>2+</sup> is critical for controlling contractility of glycerinated muscle fibers (Bozler, 1954; Watanabe, 1955, 1957), isolated myofibrillar and natural actomyosin ATPase activities (Weber et al., 1963), myofibrillar contraction (Weber, 1961, 1963) and superprecipitation of actomyosin (Weber et al., 1961; Ebashi, 1960, 1962). These observations suggested the concept that physiological Ca<sup>2+</sup> release and uptake by the SR causes muscle to contract and relax

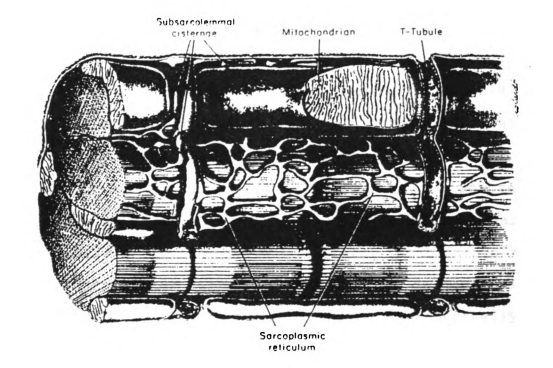


Figure 1. Schematic representation of mammalian cardiac sarcoplasmic reticulum and T-tubules (From Fawcett and McNutt, 1969, J. Cell Biol. 42, 24).

respectively.

Ca2+ release and subsequent reaccumulation by the SR takes place in each contraction and relaxation cycle (Tada et al., 1978). Both skeletal and cardiac SR accumulate calcium against a concentration gradient. However, the calcium uptake rate of the skeletal SR is higher than that of cardiac SR (Carsten, 1964; Katz et al., 1967; Harigaya et al., 1969; Suko et al., 1973). Ca<sup>2+</sup>-dependent ATPase (Ca-ATPase), 1970. represents 60-80% of total skeletal muscle SR vesicle protein (Deamer, 1973; Ikemoto et al., 1971; Inesi, 1972; Martonosi et al., 1971; Meissner et al., 1973; Yamada et al., 1971), and about 40% for cardiac SR (Tada et al., 1978; 1982) serves as a Ca2+-pump, transducing chemical energy into osmotic work during the translocation of Ca2+ across the SR membrane. The Ca-ATPase amino acid sequences of both skeletal and cardiac SR have been deduced from their cDNAs. Both proteins have relative molecular masses of about 100,000 daltons (MacLennan et al., 1975), and both are distributed asymmetrically across the SR membrane. These proteins are amphipathic single polypeptides which have their hydrophobic regions embedded in the SR membrane and most of their hydrophilic portions exposed in the cytoplasm (Tada et al., 1984).

Ca<sup>2+</sup>-ATPase functions as an energy transducer and carrier of Ca<sup>2+</sup> during the translocation of Ca<sup>2+</sup> across the SR membrane (Tada et al., 1988) and its reaction scheme is shown in Figure 2. Translocation of Ca<sup>2+</sup> is coupled with the formation of a phosphoprotein intermediate, EP, which has the terminal

phosphate of ATP incorporated into the ATPase at the  $\beta$ -carboxyl group of aspartic acid (Asp 351) at the active site, forming an acid-stable acyl phosphate (Bastide et al., 1973; Degani et al., 1973; MacLennan, et al., 1985). The maximal concentration of phosphoprotein in cardiac SR preparations is about  $\frac{1}{2}$  of that in skeletal muscle (Shigekawa et al., 1976).

The three steps in the Ca-ATPase cycle are recognition and binding of Ca2+, translocation of Ca2+ across the membrane, and release of Ca2+ into the SR lumen. In the Ca2+ uptake process (Tada et al., 1978), the enzyme recognizes Ca2+ and binds it at the cytoplasmic face of the SR membrane. ATP-energized, Ca<sup>2+</sup>-bound ATPase translocates Ca<sup>2+</sup> from outside to the inside of the membrane by forming the phosphoenzyme intermediate, EP. Finally, the translocated Ca2+ is released from the ATPase into the interior of the SR membrane as EP decomposes (Tada et al., 1978). Figure 2 is a proposed reaction scheme of the ATPase (DeMeis et al., 1979; Tada et al., 1979, 1984), where the \* indicate inside of the SR membrane. E, and E, P show higher affinity for  $Ca^{2+}$  than that of E<sub>2</sub> and E<sub>2</sub>~P. E<sub>1</sub>~P is assumed to predominate under the usual circumstances where Ca2+ and K+ are present at neutral pH. The amount of E~P represents the sum of  $E_1 \sim P$  and  $E_2 \sim P$ . Shigekawa et al. (1978) demonstrated that  $E_1 \sim P$  is reactive with ADP and forms ATP reversibly, whereas E2~P does not react with ADP to form ATP.

Differences in the rate of Ca<sup>2+</sup> uptake between cardiac and skeletal SR suggested differences in regulation of Ca<sup>2+</sup>-pumping activity in these two membranes. In the 1970's several

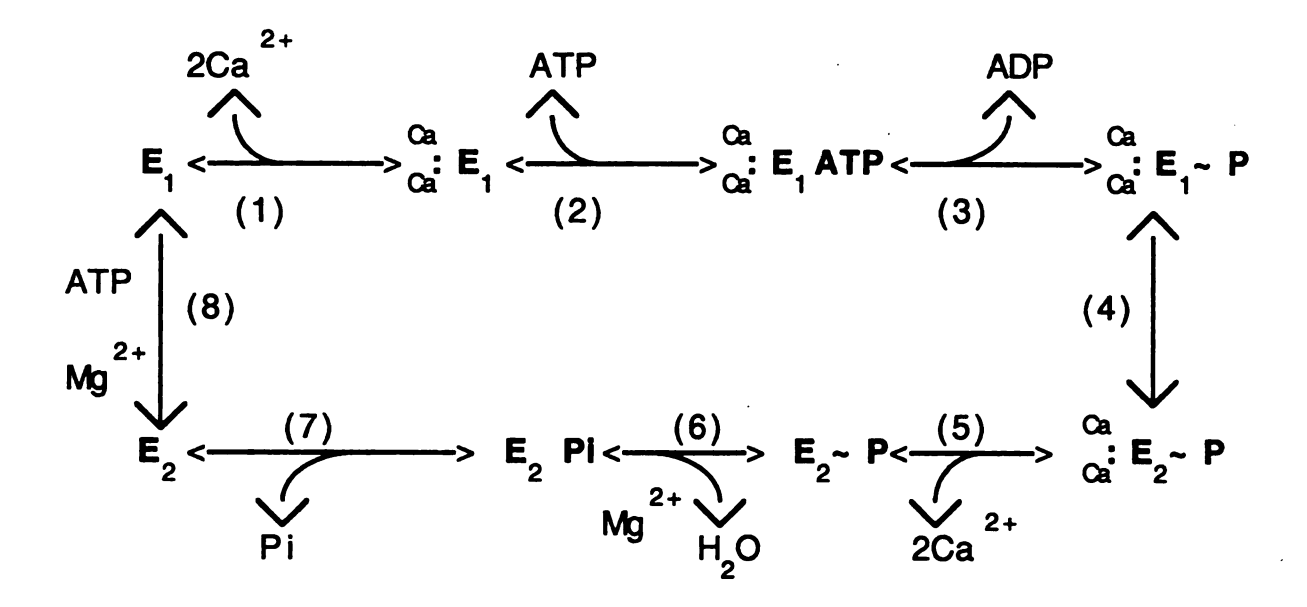


Figure 2. Reaction scheme of Ca-ATPase. E and E~P represent non-phosphorylated and phosphorylated Ca-ATPase, respectively. 1 and 2 indicate inside and outside of the SR membrane (From de Meis and Vianna, 1979, Ann. Rev. Biochem. 48, 280).

researchers suggested that a protein kinase catalyzes the phosphorylation of a SR membrane protein of Mr ~22,000 which alters the activity of the cardiac SR Ca<sup>2+</sup> pump (Tada et al., 1974; Kirchberger et al., 1974; LaRaia et al., 1974). This phosphoprotein, named phospholamban (PLB), exists in an approximate 1:1 mole ratio with the ATPase within the membrane (Tada et al., 1979, 1983).

Tada et al. (1975) demonstrated that the cAMP-dependent protein kinase catalyzes phosphorylation of PLB, which results in an increase in the rate of Ca2+ uptake by enhancing the turnover of the ATPase enzyme. Phosphorylation by the cAMPprotein kinase increases the Ca<sup>2+</sup> sensitivity of the Ca-ATPase. In other words, phosphorylation of PLB increases the rate of Ca2+ uptake of the SR at given Ca2+ concentration (Kirchberger et al., 1974; Tada et al., 1974; Katz, 1979). Tada et al. (1979, 1980) examined the effect of PLB phosphorylation by cAMP-dependent protein kinase on the steady-state kinetics of EP and P, formation. Upon phosphorylation of PLB by cAMPdependent protein kinase, the rate of the EP intermediate formation significantly decreased, whereas the rate of P. liberation increased. These results indicate that the overall turnover rate of Ca-ATPase is markedly enhanced through the increase of EP decomposition.

Later research indicated that PLB can also be phosphorylated by a calmodulin (CaM)-dependent protein kinase (LePeuch et al., 1979). In absence of phosphorylation by the cAMP-dependent protein kinase, CaM-dependent phosphorylation

is able to stimulate SR Ca<sup>2+</sup> uptake (LePeuch et al., 1979). The maximal amount of PLB phosphorylation catalyzed by CaM-dependent protein kinase is about the same as that found with cAMP-dependent protein kinase (Tada et al., 1983). The stimulatory effects of CaM-dependent protein kinase and cAMP-dependent protein kinase on Ca<sup>2+</sup> transport are additive. Phosphorylation by two kinases occurs in an independent manner, suggesting that the activity of Ca-ATPase is regulated by a dual second messenger system (Katz et al., 1978; Lopaschuk et al., 1980; Tada et al., 1983).

PLB exists in cardiac muscle, slow-contracting skeletal muscle, smooth muscle and platelets (Tada et al., 1988). PLB is a complex proteolipid composed of 5 identical subunits (Wegener et al., 1984), each consisting of 52 amino acids and each having a subunit relative molecular mass of 6,080 daltons (Simmerman et al., 1986; Fujii et al., 1987). Phosphorylation of PLB by cAMP-dependent protein kinase occurs at Ser 16, whereas phosphorylation by CaM-dependent protein kinase occurs at Thr 17 (Tada et al., 1982; Fujii et al., 1987; Simmerman et al., 1986). The first 25-30 amino acids of this protein are hydrophilic and are predicted to be exposed to the cytoplasm, whereas the remainder are hydrophobic and are thus likely to be embedded in the membrane (Simmerman et al., 1986; Fujii et al., 1987). The content of PLB in cardiac SR is about 4 to 6% (w/w) of the total protein, whereas that of ATPase enzyme is around 40% in cardiac muscle (Tada et al., 1982). The presence of several positively charged amino acids makes the protein basic (pI=10) (Jones et al., 1985).

From a biophysical point of view PLB is a unique membrane protein since several studies suggested it exerts its physiological function by direct protein-protein interaction with the Ca-ATPase (Tada et al., 1974, 1982; LePeuch et al., 1980). The direct interaction between the two proteins was first suggested by James et al., (1989). They employed the Denny-Jaffe crosslinking reagent, which consists succinimidyl group for attaching to amines, a photoacivatable azido group for crosslinking to target proteins, a cleavable diazo linker, and a radiolabel (125I) which remains with the receptor following cleavage of the crosslinker. Their results indicated that only non-phosphorylated PLB was crosslinked with ATPase by this reagent, whereas phosphorylated PLB was not crosslinked to the Ca-ATPase. These data suggest that phosphorylation of PLB results in dissociation of PLB from the Ca-ATPase. However, the submolecular characteristics of PLB and its interaction with the ATPase are still poorly understood (Tada et al., 1988). PLB is also unique from a physiological point of view because it mediates the effects of both cAMP and Ca2+ to induce the changes in contractility of myocardial cells and other cells under the influence of receptor agonists, such as β-adrenergic agents, which increase intracellular cAMP and Ca2+, respectively (Tada et al., 1982; 1983).

CaM has a relatively low molecular mass, and is an acidic  $Ca^{2+}$ -binding protein which has been identified in a wide

variety of eukaryotic cells (Cheung, 1980; Klee et al., 1980). It has a single 148 amino acid polypeptide chain which can be divided into four structurally related Ca2+-binding domains (Kretsinger, 1976; 1980). Its high-affinity Ca2+-binding sites consist of a helix-loop-helix structure which consists of 12 amino acid residues. The four helix-loop-helix structures are connected by eight to nine residues of random coil (Kretsinger, 1976; 1980). CaM possesses approximately 63% αhelical content in the absence of Ca2+; binding of Ca2+ results in a small further increase in the q-helical content, as well as a tertiary structural change which exposes two hydrophobic patches to the solvent (Babu et al., 1985). This Ca2+-induced conformational change allows CaM to interact with modulate the activities of numerous enzymes and peptides including multifunctional CaM-dependent protein kinases, NAD kinase, phosphodiesterase, plasmalemma calcium pumps as well as proteins involved in motility and cell division (Klee and Vanaman, 1982; Means et al., 1991).

Cox et al. (1985) suggested that a structural feature common to many CaM-binding proteins is a basic amphiphilic helix which shares amino acid sequence homology with the cytotoxic peptide from bee venom, melittin. Melittin is a 26 amino acid peptide which has been used as a model peptide for studying CaM binding. Melittin has a primary structure in which 2-3 hydrophobic residues separate a cluster of hydrophilic residues along the helix, such that a hydrophobic patch exists on one face of the helix. Calmodulin also

contains 2 hydrophobic patches which become more exposed upon calcium binding.

A CaM-binding fragment of skeletal muscle myosin light chain kinase (MLCK) shows considerable sequence homology with CaM-binding peptides, such as melittin (Blumenthal et al., 1985). Other studies proposed CaM-binding domains of smooth muscle (Lukas et al., 1986) and skeletal muscle (O'Neil et al., 1987) MLCK could form a basic amphiphilic  $\alpha$ -helix. Recent NMR studies of CaM-MLCK complexes suggested that the  $\alpha$ -helical linker which connects the two globular lobes of CaM may bend and let the hydrophobic faces of the two lobes contact the hydrophobic faces of the MLCK helix (Ikura et al., 1992; Kretsinger, 1992).

The subunits of PLB have the potential to form an amphiphilic helix in the 30-residue N-terminal, hydrophilic region protruding from the SR membrane. The hydrophilic fragment is characterized by clusters of positively charged amino acids separated by hydrophobic residues (Figure 3). This polypeptide displays a typical amphiphilic  $\alpha$ -helical conformation with most of the hydrophobic amino acids on one side of the helix and the positively charged residues on the other (Simmerman et al., 1989).

The interaction between PLB and CaM was first suggested through affinity labeling studies directed at identification of the CaM-dependent protein kinase (Louis and Jarvis, 1982). CaM was labeled with <sup>125</sup>I, incubated with SR vesicles, and covalently cross-linked to its target proteins upon addition

of the bifunctional cross-linker, dithiobis(succunimidyl propionate), which links proximal lysine groups. The cross-linked products were separated by polyacrylamide gel electrophoresis and identified by autoradiography. Instead of finding a CaM + CaM-dependent kinase complex, Louis and Jarvis (1982) observed a 1:1 cross-link between CaM and PLB. Their studies identified PLB, the kinase substrate, rather than the CaM-dependent kinase, as the major CaM receptor in cardiac longitudinal SR.

In their study, any lysine residue of CaM which would be close to a lysine a receptor of CaM to PLB (Lys 3) could be crosslinked. However, since this method requires that both near each other and oriented correctly, lvsines be crosslinking of CaM to kinase may not have occurred. In subsequent studies, Strasburg et al. (1988) purified wheat germ CaM, which has a single sulfhydryl group (Cys 27) in Ca2+binding domain I. They iodinated protein at the sole tyrosine residue and site-specifically labeled it at Cys 27 with the photoactivatable crosslinker, benzophenone maleimide which could crosslink any proximal amino acid of a receptor protein. This CaM derivative was incubated with SR vesicles, photolyzed and the cross-linked products were characterized. obtained similar results to that of Louis and Jarvis (1982).

Although these studies did not prove that CaM binds to PLB, they did show that PLB is within 8Å of the Cys in the N-domain of CaM, and they suggested that CaM might bind to PLB to form a 1:1 complex. This binding could play an important

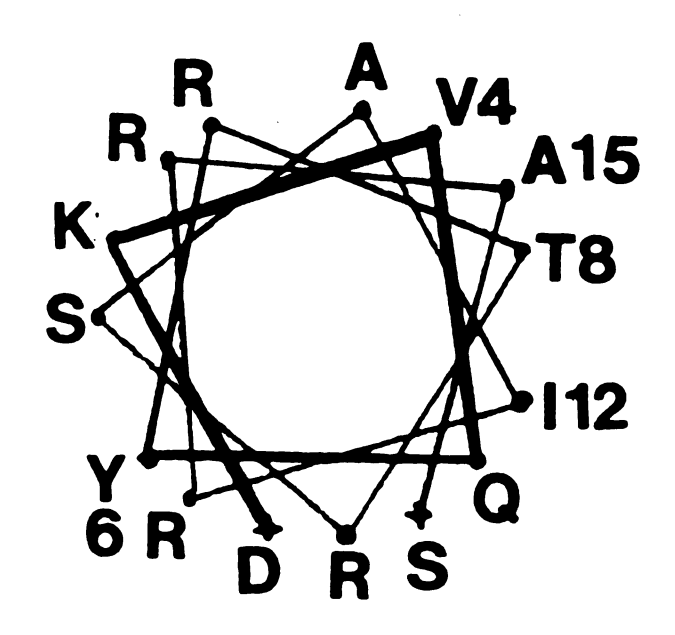


Figure 3. Helical wheel diagram of phospholamban residues 2-16. It is characterized as an amphiphilic,  $\alpha$ -helical portion of PLB. The hydrophobic cluster consists of Val 4, Thr 8, Ile 12 and Ala 15 (From Gao, Levine, Mornet, Slatter and Strasburg, 1993, Biochim. Biophys. Acta, 1160, 29).

role in activating CaM-dependent protein kinase for phosphorylation of PLB and thus could indirectly increase the Ca<sup>2+</sup> uptake rate of the SR.

Recent studies have focused on the molecular mechanism of regulation of the CaM-dependent protein kinase. Hanson et al. (1988) showed that removal of the N-terminal 6 amino acids from PLB in SR vesicles by limited chymotryptic digestion resulted in decreased CaM-dependent phosphorylation of PLB. The decrease in CaM-dependent phosphorylation paralleled the decrease in benzophenone-125I-calmodulin and disuccinimidyl suberate plus 125I-calmodulin crosslinking of PLB in SR vesicles. However, cAMP-dependent phosphorylation of PLB was unaffected. Similarly, limited proteolysis of endoproteinase Lys-C (which cleaves at the C-terminal side of Lys-3), resulted in decreased CaM-dependent phosphorylation, and benzophenone-CaM and dissuccinimidyl suberate-CaM crosslinking, whereas cAMP-dependent crosslinking was unaffected. These results suggest that the first 3-6 residues of PLB are essential in the formation of a CaM-PLB complex which could be part of the mechanism of activation of the endogenous SR CaM-dependent protein kinase.

The first specific aim of this study was to define the domain(s) of CaM which interact with PLB. The second specific aim was to characterize the affinity of the CaM-PLB complex using a synthetic peptide corresponding to the cytoplasmic half of PLB in order to determine whether the interaction with CaM may be physiologically significant. The third specific aim

was to localize the portion of PLB interacting with CaM which regulates the activity of CaM-dependent protein kinase. The information derived from these experiments will be useful in defining the mechanism of regulation of CaM-dependent phosphorylation of PLB and therefore, of Ca<sup>2+</sup> regulation in muscle cells.

#### **FLUORESCENCE**

Luminescence is the emission of photons from electronically excited states. In the singlet state, the electron in the higher energy orbital has the opposite spin orientation to that of the second electron in the lower orbital. These two electrons are paired. In a triplet state these electrons are unpaired and their spins have the same orientation. Fluorescence is the emission of photons which results from the return to the lower orbital of the paired electron. Such emission rates are typically near 10° sec-1. These high emissive rates result in fluorescence lifetimes near 10<sup>-8</sup> sec or 10 nsec. On the other hand, phosphorescence is the emission of photons which is caused by the transition between triplet excited states returning a singlet ground emissive rates state. Such slow and the typical are phosphorescence lifetimes range from milliseconds to seconds. In general, compounds that fluoresce or phosphoresce contain either electron-donating groups (amines, alcohol and hetero atoms) or multiple conjugated double bonds (aromatic rings).

The absorption and emission of light is illustrated by the energy-level diagram suggested by Jablonski (1935) (Figure 4). It generally requires radiation energy in the ultraviolet and visible region to raise one of singlet state electrons to an excited state ( $S_0$  to  $S_1$  or  $S_0$  to  $S_2$ ). Some of the molecules in

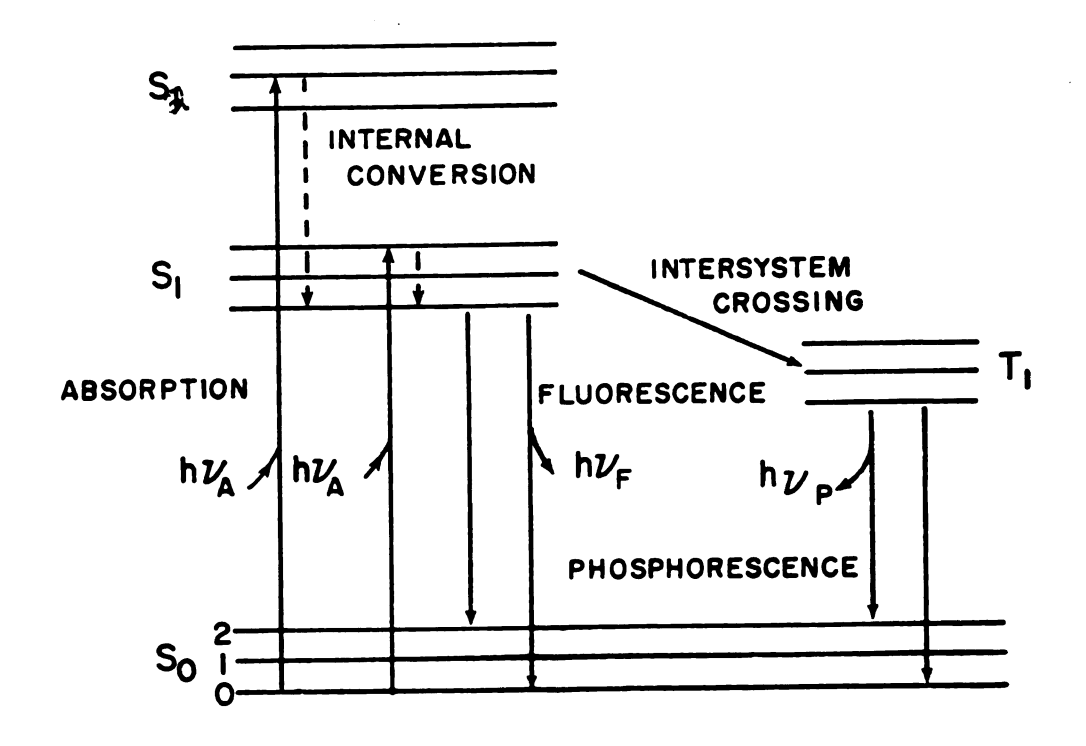


Figure 4. Schematic energy-level diagram (From Lakowicz, Principles of Fluorescence Spectroscopy, 4).

condensed phases rapidly return to the lowest vibrational level of  $S_1$ . In this process, the energy can be absorbed by the solvent and no radiation is given off. If the electron returns to the ground state with the emission of radiation ( $S_1$  to  $S_0$ ) the process is called fluorescence. This emitted energy is usually in the visible or near infrared region. However, the energy emitted is less than that originally absorbed.

Intersystem crossing is the process of changing from the singlet state to a triplet state ( $S_1$  to  $T_1$ ). This process can be very fast (about  $10^{-8}$  sec) and is enhanced by the presence of heavy atoms within the molecule. After intersystem crossing, the molecule goes to the lowest vibrational level of the triplet state by vibrational relaxation in  $10^{-13}$  sec. When the molecule drops from the triplet state to the ground state phosphorescence is emitted.

The spectrofluorometer is an instrument for measurement of fluorescence. Figure 5 shows a schematic diagram of a general spectrofluorometer. The radiation source can be in the ultraviolet or visible range. Hydrogen, deuterium, mercury and xenon lamps are commonly used as a light source. The basic components are similar to those of ultraviolet/visible spectrophotometer.

The instrument shown is equipped with monochromators to select both the excitation and emission wavelengths. The main difference between a fluorometer and a spectrophotometer is that the detector is at a right angle to the incident radiation in a fluorometer, so that little of the incident

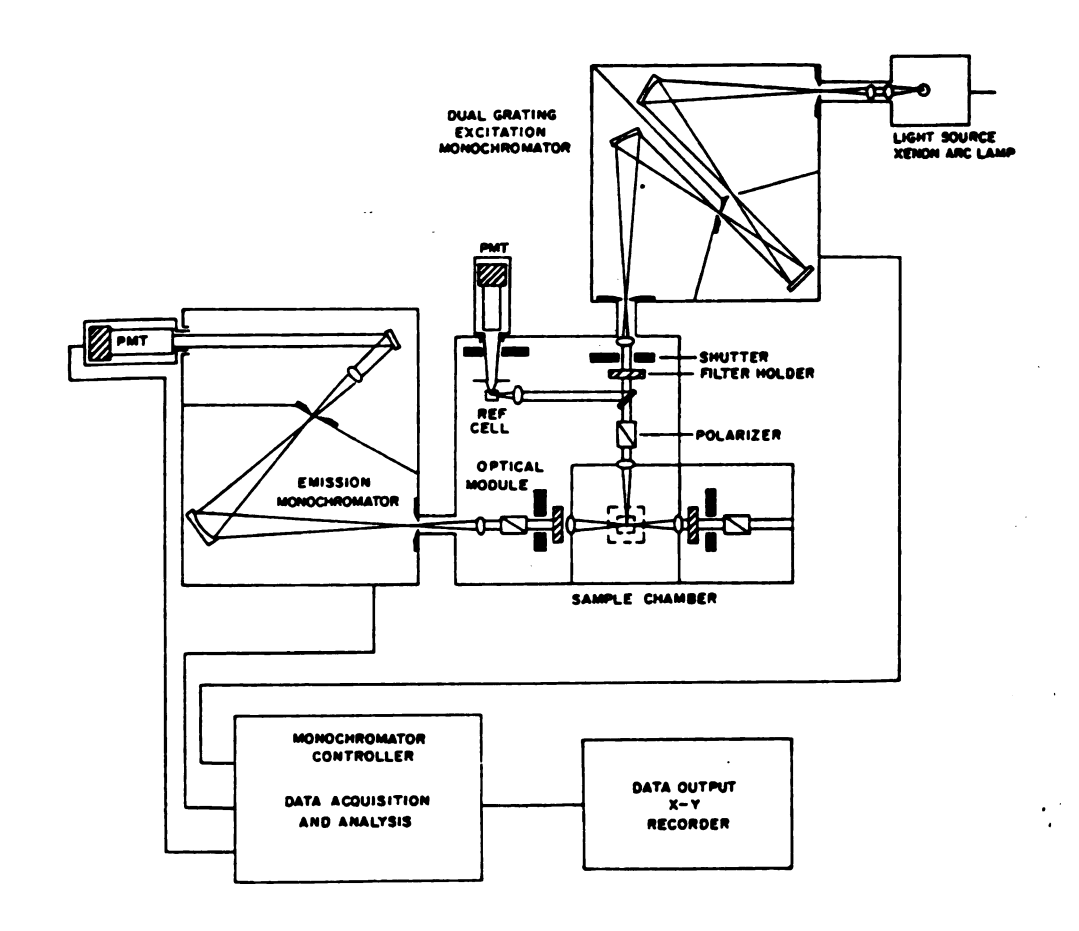


Figure 5. Schematic diagram of the components of a spectrofluorometer (From Lakowicz, Principles of Fluorescence Spectroscopy, 21).

radiation will strike the detector. If there is no luminescence, the detector will register zero signal since only light emitted from sample reaches the detector. An increase in signal indicates an emission from the sample.

The excitation monochromator is used to isolate a narrow band of electromagnetic radiation from the light source. There are two types are used in fluorescence equipment: filters and gratings. The latter type of instrument was used in this study. A grating consists of a large number of parallel lines or grooves ruled at extremely close intervals (e.g., 30,000) lines per inch) on a highly polished surface, such as \_aluminum. When a beam of monochromatic light is focused on a transmission grating, each line acts like a source of this radiation. At certain points on the opposite side of the grating the wavelengths reinforce each other. At other points there is destructive interference and darkness. The result is a series of bright lines with dark regions between them. The polychromatic radiation passing through the grating due to their own diffraction angle is separated into a spectrum. The typical diffraction grating as shown in Figure 6 has two important factors: blaze angle and the number of lines or grooves in the grating. The basic equation for a grating is

 $n \lambda = 2 d \sin\theta$ ....(1)

where n is the order of diffraction, d is the distance between wavelength of the radiation.  $n\lambda=0$  when radiant energy strikes

adjacent grooves,  $\theta$  is the angle of reflectance and  $\lambda$  is the the grating so that the angles of incidence and diffraction are equal but opposite in sign. This is the zero order spectral reflection in a reflection grating.

The resolving power R of a grating is given as

$$R = \frac{\lambda}{\Delta \lambda} = mN....(2)$$

where  $\Delta\lambda$  is the wavelength difference between two lines that are barely distinguished,  $\lambda$  is their average wavelength, m is the length of the grating in centimeters and N is the number of lines or grooves in the grating. The greater the number of lines, the greater the resolution. The more lines per unit length, the greater the dispersion in the first order. The fluorometer used for this research contains two gratings which increases the purity of the exciting wavelength. In addition, these monochromators use concave gratings produced by holographic means, which further decrease stray light. Since imperfections of the gratings are the major source of stray light transmission by the monochromators, and of ghost images from the grating. For this reason the holographic gratings are preferable for fluorescence spectroscopy. Both monochromators are motorized to allow automatic scanning of wavelength.

The transmission efficiency of grating monochromators is a function of wavelength. The efficiency at any given wavelength can be maximized by choice of the blaze angle with mechanically produced gratings. Generally, an excitation monochromator has high efficiency in the ultraviolet and emission monochromator has high efficiency in the visible region. However, holographic gratings are not blazed but the shape of the grooves can be varied. Their peak transmission is less efficient than a planar grating with mechanically produced gratings. On the other hand, the efficiency is more widely distributed on the wavelength scale than that of planar gratings.

Most fluorometers use photomultiplier tubes (PMT) as detectors. A PMT consists of a photocathode and a series of dynodes which are amplification stages. The photocathode is a thin film of metal on the inside of the window. Incident photons cause electrons to be ejected from this surface. Both the photocathode and the dynodes are held at negative potentials, but the potentials decrease towards zero along the dynode chain. The photocathode-to-first-dynode potential is generally fixed at a constant voltage by a Zener diode at values ranging from -50 to -200V. The potential difference between the photocathode, which is typically -1,000 to -2,000V, and the first dynode causes an ejected photoelectron to be accelerated towards the latter. Upon collision with the first dynode the photoelectron causes 5 to 20 additional electrons to be ejected, depending on the voltage difference to this dynode. This process continues down the dynode chain until the current pulse arrives at the anode. The intensity of this pulse depends upon the overall voltage applied to the PMT. Higher voltage results in the greater numbers of

electrons ejected from each dynode and gives higher amplification.

Figure 5 also shows a number of convenient features of this instrument. Shutters are provided to eliminate the exciting light or to close off the emission channel. A beam splitter is provided in the excitation light path and reflects part of the excitation to a reference cell, which generally has a stable reference fluorophore. Changes in intensity of the lamp may be corrected for by division of the intensity from the sample by that of the reference fluorophore. Polarizers in both excitation and emission light paths are removable so that they can be inserted only for measurements of fluorescence anisotropy or for selection of particular polarized components of the emission and/or excitation.

The emission of light from fluorescent samples can be polarized upon excitation with polarized light. Fluorophores are selectively excited or photoselected according to the orientation of their dipoles relative to the direction of the polarized excitation light. The emitted light from the photoselected probes will therefore be polarized if the emission occurs before rotation of the molecule has occurred. Polarization or anisotropy measurements demonstrate the average angular displacement of the fluorophore which occurs between absorption and subsequent emission of a photon. The angular displacement is dependent upon the rate and extent of rotational diffusion during the lifetime of the excited state. Rotational diffusion, in turn depends on the viscosity of the

solvent and the size and shape of the fluorescent species.

Polarization (P) and anisotropy (r) are defined as

$$P = \frac{I_{I} - I_{\perp}}{I_{I} + I_{\perp}}$$
 (3)

$$r = \frac{I_I - I_{\perp}}{I_I + 2I_{\perp}}$$
 (4)

The polarization (P) and anisotropy (r) are defined as

$$P = \frac{3r}{2+r} \tag{5}$$

$$r = \frac{2P}{3-P} \tag{6}$$

Measurement of fluorescence anisotropy has been widely utilized to quantify the association reactions between biological molecules, e.g. antigen-antibody binding (Levison, 1975), the association between proteins (Rawitch and Weber, 1972) and the association of ligands with proteins and nucleic acids (Visser and Lee, 1980; Ellerton and Isenberg, 1969).

The relationship of measured fluorescence anisotropy with the fraction of free (F) and bound(B) fluorophore is defined as:

$$r=f_Fr_F+f_Br_B$$
....(7)

where  $r_r$  and  $r_s$  are the anisotropies of the free and bound fluorophores and  $f_r$  and  $f_s$  refer to the fraction of the total fluorescence which is due to each form of the fluorophore. Thus,  $f_r + f_s = 1$ .

The equilibrium of a ligand (L) binding to a protein (P) is defined as:

$$L + P = PL$$
....(8)

The dissociation constant K for this reaction is given by

$$K = \frac{[P][L]}{[PL]}...(9)$$

The fraction of bound ligand is

$$f_B = \frac{[PL]}{[L_o]} = \frac{[P]}{[P] + K}$$
....(10)

where  $[L_0]=[L]+[PL]$  is the total concentration of ligand. Since the quantum yield may change upon binding, to take this change into account we get

$$f_B = \frac{r - r_F}{(r_R - r)R + r - r_F}$$
....(11)

where R is the ratio of the quantum yield of the bound and the free form. When R=1, Equation 18 reduces to:

$$f_B = \frac{r - r_F}{r_B - r_F}$$
....(12)

Generally the values of  $r_r$  and  $r_s$  can be obtained by measuring anisotropy of the fluorescent ligand in the absence of protein and at significantly high protein concentration which is adequate to bind all the fluorophore, respectively. Then the fraction of free  $(f_r)$  and bound  $(f_s)$  ligand can be calculated from any measured value of  $r_s$ .

There are many biological molecules contain naturally

occurring or intrinsic fluorophores, such as, tryptophan, riboflavin, etc. However, sometimes the natural fluorescence properties of macromolecules are not adequate for the desired experimentation. For instance, protein intrinsic polarization fluorescence. and even the of fluorescence, may not be sensitive to the phenomenon one wishes to quantify. Or, the presence of multiple fluorophores in a protein may make interpretation difficult. Extrinsic fluorescence probes are chosen for protein labeling to circumvent the problem associated with intrinsic fluorescence measurements. Rhodamine-X-maleimide and N - ((2 -(iodoacetoxy)ethyl-N-methyl)-amino-7-nitrobenz-2-oxa-1,3 diazole) (IANBD), which are two probes frequently used to label the sulhydryl group of proteins were utilized in this study. The lifetime of rhodamine is near 4 nsec and its spectrum is not significantly sensitive to solvent polarity which can change the quantum yield of the fluorophore. It is suitable for quantifying the associations of small labeled molecules via changes in fluorescence polarization. IANBD tends to be more sensitive to changes its environment and thus provides complementary information to that of rhodamine-Xmaleimide.

#### MATERIALS AND METHODS

#### I. MATERIALS

Longitudinal or free SR vesicles from pig heart muscle were prepared by the method of Kirchberger (1974) and stored in 10% sucrose at -70°C. A peptide corresponding to residues 1-25 of phospholamban was synthesized by the Macromolecular Structure Facility of Department of Biochemistry, Michigan State University. AT32P was purchased from Du Pont New England Nuclear (Boston, MA). Wheat germ CaM was purified from untoasted wheat germ purchased from a health food store using a procedure based on that of Yoshida (1983) and modified by Strasburg et al. (1988). Mutant Q143C CaM (site-directed mutant of chicken CaM which has Cys at residue 143 instead of Gln) was obtained from Dr.C.L.A. Wang of Boston Biomedical Research Institute. The fluorescence probes (rhodamine-X-N-((2(iodoacetoxy)ethyl-N-methyl)-amino-7maleimide and nitrobenz-2-oxa-1,3-diazole (IANBD) were purchased from Molecular Probes (Eugene, OR). a-Chymotrypsin, cAMP, cAMPdependent protein kinase, and melittin were purchased from Sigma Chemical Co. (St. Louis, MO).

#### II. METHODS

#### (1) Preparation of Cardiac Light SR Vesicles:

Trimmed pig heart muscle was homogenized in a Waring

Blendor with 5 ml of Medium I [(10 mM NaHCO3, 1 mM ethylene glycol-bis( $\beta$ -aminoethyl ether) (EGTA)] per gram of muscle and centrifuged at 7,500 rpm  $(9,000 \times g_{max})$  for 10 minutes in a The supernatant was collected and Sorvall GSA rotor. centrifuged again in the same rotor at 7,500 rpm  $(9,000 \times g_{max})$ for 20 minutes. The pellet was discarded and the supernatant was centrifuged for 30 minutes at 31,000 rpm (100,000 x  $g_{max}$ ) in a Beckman Type 35 rotor. The pellets were resuspended in Medium II (0.6 M KCl and 20 mM Tris, pH 6.8) and centrifuged at 39,000 rpm (155,000 x  $g_{max}$ ) for 40 minutes in a Beckman Type 70 rotor. The pellet was resuspended in 20 ml of Medium III (0.3 M sucrose, 0.4 M KCl, 5 mM piperazine-N,N'-bis[2ethanesulfonic acid (PIPES), pH 6.8, 0.1 mM MgCl2, 0.1 mM EGTA and 0.1 mM CaCl2) and 5 ml aliquots were loaded on each of four sucrose density gradients. The sucrose gradients consisted of four fractions of increasing density: Fraction 1 (21.6% w/v sucrose), Fraction 2 (32.6% w/v sucrose), Fraction 3 (36.4% w/v sucrose) and Fraction 4 (40.4% w/v sucrose). After centrifugation for 4 hours in a Du Pont AH629 rotor at 25,000 rpm (120,000 x  $g_{max}$ ), light SR vesicles were localized at the interface of Fractions 1 and 2. The collected light SR was diluted with two volumes of Medium IV (10% sucrose) and centrifuged for 40 minutes at 35,000 rpm (130,000 x  $g_{max}$ ) in a Beckman Type 70 rotor. The pellet was resuspended in a minimal amount of Medium IV and stored at -70°C. The protein content was measured by the Lowry-Folin assay (Lowry et al., 1951).

### (2) Preparation of Wheat Germ CaM:

Three hundred gram of untoasted wheat germ were blended in a Waring Blendor and extracted three times each with 1 liter of acetone. The residue was air-dried and mixed with 2 liters of 50 mM NaH<sub>2</sub>PO<sub>4</sub>, pH 5.9, 5 mM Na<sub>2</sub>EGTA, 0.1 mM phenylmethylsulfonyl fluoride (PMSF), 30 mM 2-mercaptoethanol. The suspension was homogenized with a Brinkman Polytron for three one-minute bursts, with 5-minute rests between bursts, and stirred for three hours at 4°C. The suspension was centrifuged at 12,000 rpm (23,000 x g<sub>max</sub>) in a Sorvall GSA rotor for 25 minutes. The supernatants were pooled and the volume was measured trichloroacetic acid (TCA) (50% w/v) was slowly added at 0°C to a final concentration of 3% based on the following formula:

Volume of 50% 
$$TCA = \frac{(Final\%) - (Initial\%)}{50\% - (Final\%)} \times Volume of Supernatant.....(13)$$

The pH was adjusted to 5.2 with Tris base, and the suspension was stirred for one hour. The suspension was centrifuged for 20 minutes at 12,000 rpm (23,000 x  $g_{max}$ ) in a Sorvall GSA rotor and the supernatant was adjusted to a final TCA concentration of 5% using Equation 1. This suspension was centrifuged for 10 minutes at 10,000 rpm (16,000 x  $g_{max}$ ) in a Sorvall GSA rotor.

The pellet was suspended in about 100 ml of 1 M N-(2-hydroxyethyl)piperazine-N'-(2-ethanesulfonic acid (HEPES), pH 7.5 and adjusted to pH 7.5 with Tris base. Solid ammonium sulfate was slowly added to the protein suspension to a final

saturation of 55% at 0°C, and the suspension was stirred for an additional 30 minutes and centrifuged for 90 minutes at 20,000 rpm  $(41,000 \times g_{max})$  in a Beckman Type 70 rotor. The supernatant was adjusted to 5 mM CaCl, and applied to a phenyl-Sepharose column equilibrated with 25 mM HEPES, pH 7.5, 0.1 mM CaCl, and 15 mM 2-mercaptoethanol. The column was washed with this buffer until  $A_{280}$  returned to baseline. The column was washed with 0.5 M NaCl, 25 mM HEPES, pH 7.5, 0.1 mM 15 mM 2-mercaptoethanol until the absorbance CaCl, and returned to baseline. Calmodulin was eluted with 25 mM HEPES, pH 7.5, 15 mM 2-mercaptoethanol and 2 mM EGTA. The calmodulincontaining fractions were pooled and dialyzed three times vs 2 liters of 1 mM ammonium bicarbonate and lyophilized. Purity of the calmodulin was checked by SDS polyacrylamide gel electrophoresis.

#### (3) Fluorescent Labeling of Q143C CaM:

Two mg of wheat germ or Q143C CaM were dissolved in 1 ml of 6 M guanidine hydrochloride, 25 mM HEPES, pH 7.5 and 2 mM EDTA. Solid DL-dithiothreitol (DTT) was added to give a final concentration of 10 mM. After incubation at room temperature for 30 minutes, the protein was rapidly desalted using ultrafiltration. The solution was concentrated to 100  $\mu$ l with Centricon 10 concentration. The concentrate was adjusted to 2 ml with 1 mM HEPES, pH 7.5 and again concentrated to 100  $\mu$ l. This was repeated twice and the volume was then adjusted to 1 ml with 1 mM HEPES, pH 7.5. The concentration of CaM in mg/ml was determined by the formula  $(A_{280}-A_{120})/0.18$ .

One mg of the fluorescent reagent, IANBD or rhodamine-Xmaleimide, was dissolved in 1 ml dimethylformamide. HEPES buffer, pH 7.5, ethylenediaminetetraacetic acid (EDTA), and guanidine hydrochloride were added to final concentrations of 50 mM, 2 mM, and 6 M, respectively. Five moles of fluorescent reagent were added per mole of CaM, and the tube was placed on an orbital stirrer and mixed for 4 hours at room temperature. reaction was stopped by adding DTT to a concentration of 10 mM. The labeled CaM was dialyzed once against 2 liters of 5 mM PIPES, pH 6.8 and 1 mM EDTA and concentrated to 0.5 ml. The concentrate was applied to a Sephadex G-25 column equilibrated with 0.3 M KCl, 20 mM HEPES, pH 7.5 and 1 mM EDTA to remove any adsorbed fluorescent label. The labeled CaM was scanned from 650 nm to 250 nm and the stoichiometry of labeling of CaM was calculated based on the extinction coefficients of 82,000 M<sup>-1</sup>cm<sup>-1</sup> at 580 nm for rhodamine-X-maleimide and 26,000 M<sup>-1</sup>cm<sup>-1</sup> at 490 nm for IANBD. The concentration of CaM was measured using the bicinchoninic acid assay (BCA) with unlabeled CaM as the standard (Smith, et al., 1985).

### (4) Fluorescent Labeling of Wheat Germ CaN

The procedure for labeling wheat germ CaM is the same as that for Q143C CaM except that the concentration of CaM in mg/ml was determined using the equation  $(A_{280}-A_{320})/0.11$ , and the reaction time was 6 hours instead of 4.

# (5) Localization of the PLB Binding Site on CaM and Affinity Study between Two Proteins:

All the fluorescence intensity and anisotropy measurements were conducted with a SLM 4800 fluorometer. The excitation wavelengths for rhodamine-X-maleimide and IANBD were 580 nm and 490 nm, respectively. Emission wavelengths were set at 605 nm for rhodamine-X-maleimide and 537 nm for IANBD for fluorescence intensity measurement. Schott RG-630 filters were used for measuring the fluorescence anisotropy of rhodamine-X-maleimide.

# Titration of fluorescent labeled wheat germ and Q143C CaM with PLB peptide:

One  $\mu$ M fluorescence-labeled wheat germ or Q143C CaM in 20 mM PIPES, pH 7.0 and 0.1 mM CaCl<sub>2</sub> was titrated with increasing concentration of the synthetic peptide corresponding to PLB 1-25 until saturation was reached.

#### Titration of IANBD-labeled Q143C Cam with melittin:

Twenty nM IANBD-labeled CaM in 20 mM PIPES, pH 7.0, 0.1 M NaCl and 0.1 mM CaCl<sub>2</sub> was titrated with melittin until saturation was reached.

# Titration of IANBD-labeled Q143C CaM with phosphorylated PLB peptide:

One mg/ml of PLB peptide was phosphorylated by cAMP-dependent protein kinase in 50 mM PIPES, pH 7.0, 0.1 mM CaCl<sub>2</sub>, 10 mM MgCl<sub>2</sub>, 10  $\mu$ M cAMP, 0.1 mg/ml protein kinase and 1 mM ATP. The reaction was stopped by adding 20  $\mu$ l of 10 mM EGTA and 1 mM 5,5'-dithiobis-(2-nitrobenzoic acid) (DTNB). The

titration was conducted in 20 mM PIPES, pH 7.0 and 0.1 mM CaCl<sub>2</sub>.

#### Salt dependency of CaM-PLB interaction:

One  $\mu$ M IANBD-labeled Q143C CaM was titrated with KCl in the presence or absence of 30  $\mu$ M PLB peptide. The buffer conditions were 20 mM PIPES, pH 7.0 and 0.1 mM CaCl<sub>2</sub>.

#### Data analysis:

The interaction of a ligand with a protein to form a complex perturbs the conformation of both the protein and the ligand. The dissociation constant,  $K_d$ , can be defined as

$$K_d = \frac{(n[P_T] - [L_B])([L_T] - [L_B])}{[L_B]}....(14)$$

Where n is the number of binding sites on the protein molecule,  $P_T$  is total protein concentration,  $L_T$  is total ligand concentration and  $L_B$  is the concentration of bound ligand. Since  $(n[P_T]-[L_B])$  is the concentration of unoccupied binding sites while  $([L_T]-[L_B])$  is the free ligand concentration. If  $[L_T]$  is much greater than  $[P_T]$ , Equation 14 becomes

$$K_d = \frac{(n[P_T] - [L_B)[L_T]}{[L_B]}....(15)$$

Rearranging Equation 15 yields:

$$\frac{[L_B]}{n[P_T]} = \frac{[L_T]}{K_d + [L_T]}....(16)$$

To exchange  $n[P_T]$  with  $[L_T]$  the following equation is obtained

$$\frac{[L_B]}{[L_T]} = \frac{n[P_T]}{K_d + n[P_T]}....(17)$$

In this study it is assumed that there is only one binding site on CaM for PLB, since CaM tends to form a 1:1 complex with its target proteins, such as melittin (Cox et al., 1985). Therefore, the value of n is 1. In perturbation methodology,  $[L_B]$  cannot be measured directly. It is assumed that the perturbation of a protein at a finite ligand concentration is proportional to  $[L_B]$  and at infinite ligand concentration to  $n[P_T]$ . If the conformative response of a protein to the binding of a ligand is defined as  $\delta$ , and the maximum response is  $\delta_{max}$ , it follows that

$$\frac{\delta}{\delta_{\text{max}}} = \frac{[L_B]}{n[P_T]}....(18)$$

The fraction of bound CaM ( $L_B$ ) can be calculated with Equation 18 by assuming that the CaM forms a 1:1 complex with PLB (n=1). Subtracting the bound peptide concentration from the total, we can get the free ligand concentration,  $L_F$ . Plotting  $L_B/L_F$  versus  $L_B$  yields the Scatchard plot which gives the x intercept as the maximum binding capacity ( $B_{max}$ ) of the peptide to the CaM. The negative reciprocal of the slope is the

dissociation constant (K<sub>d</sub>).

(6) Localization of the Portion of PLB which Interacts with CaM:

#### Digestion of synthetic peptide:

2.5  $\mu$ g of synthetic peptide was digested by 0, 2, 5, 10, 15, 20  $\mu$ g/ml of  $\alpha$ -chymotrypsin in 25  $\mu$ l of 40 mM NaCl and 120 mM imidazole, pH 6.8 at 25°C. The reaction was stopped by adding 2  $\mu$ l of 100 mM PMSF.

The digested PLB peptide was purified by reverse-phase HPLC using a Vydac C<sub>18</sub> column. The column was equilibrated with 0.1% trifluoroacetic acid (Buffer A). The gradient for eluting the peptides was created by 0.1% trifluoroacetic acid and acetonitrile/0.1% trifluoroacetic acid (Buffer B). The gradient conditions were: (1) 5 minutes of Buffer A; (2) minutes of Buffer B; (3) 25 minutes of 20% to 30% Buffer B. The flow rate was 1 ml/min. and the absorbance was observed at 280, 254, 230 and 214 nm. The eluted fractions which corresponding to each peak were collected manually.

### Phosphorylation of PLB peptide by CaM-dependent-/cAMP-dependent protein kinase:

Digested peptide (5  $\mu$ g) was incubated in media for phosphorylation by CaM-dependent protein kinase (20 mM HEPES, pH 6.8, 10 mM MgCl<sub>2</sub>, 0.1 mM CaCl<sub>2</sub>, 1  $\mu$ M wheat germ CaM, 1 mg/ml light SR and 0.1 mM AT<sup>32</sup>P) and stopped by adding 10 mM EGTA and 1 mM DTNB. Phosphorylated peptide was separated from SR vesicles by centrifuging at 50,000 rpm (109,000 x  $g_{max}$ ) in a

Beckman TLA 100.3 rotor for 20 minutes. The supernatants were separated from the pellets. The pellets were resuspended in 90  $\mu$ l of water. Both supernatant and resuspended pellets were adjusted to a final concentration of 1% SDS, 2 mM EGTA, 10% glycerol and 0.1% bromophenol blue and loaded on a 20% polyacrylamide gel (Laemmli, 1970).

cAMP-dependent phosphorylation of the PLB(1-25) peptide was conducted in 20 mM HEPES, pH 6.8, 10 mM MgCl<sub>2</sub>, 0.15 M NaCl, 2 mM EGTA, 10 mM cAMP, 0.1 mg/ml protein kinase and 0.1 mM AT<sup>32</sup>P and stopped by adding 10 mM EGTA and 1 mM DTNB. The reactants were added to a final concentration of 1% SDS, 2 mM EGTA, 35% glycerol and adequate amount of bromophenol blue loaded on a 20% polyacrylamide gel.

The gels were stained with Coomassie blue and sandwiched with cellophane. The Easy Breeze gel dryer was utilized for air-drying the gel. Phosphorylated synthetic peptide was identified by autoradiography using Kodak Omat AR5 X-ray film. To quantitate the extent of phosphorylation, the gel bands were cut out and counted by liquid scintillation counter.

#### RESULTS AND DISCUSSION

Phospholamban (PLB) was suggested to be a major receptor of calmodulin (CaM), the activator of the CaM-dependent protein kinase in cardiac longitudinal sarcoplasmic reticulum (SR). The first study of CaM affinity-labeling in cardiac free SR vesicles (Louis et al., 1988) showed that <sup>125</sup>I-labeled CaM forms a 1:1 crosslink with PLB in the presence of the crosslinker dithiobis(succinimidyl propionate, DSP). Since DSP can span at least 8Å, their results only suggested that the two proteins are very close to each other, but they are not necessarily bound to each other. Subsequently, Strasburg et al. (1988) obtained similar results using a site-specific CaM derivative.

Hanson et al. (1988) showed that cleavage of the first 6 residues of PLB with chymotrypsin decreased CaM affinity labeling as well as CaM-dependent phosphorylation, whereas cAMP-dependent phosphorylation remained unchanged. Therefore, to define the mechanism of CaM action, it is necessary to first locate the PLB binding domain of CaM, then determine the affinity of these two proteins, and finally study the mechanism for regulating activity of CaM-dependent protein kinase by identifying the portion of PLB binds to CaM. These are the three major purposes of this study.

To identify the PLB binding domain of CaM, fluorescence

spectroscopic techniques were utilized. Wheat germ CaM, which has a single cysteine at residue 27 in the N domain, was labeled with the fluorescent probe rhodamine-X-maleimide. One um rhodamine-X-maleimide-labeled wheat germ Cam was titrated with increasing concentration of a synthetic peptide corresponding to residues 1-25 of PLB. The fluorescence intensity was measured at 605 nm as a function of PLB peptide concentration. The fluorescence intensity did not change significantly over the examined concentration range (Figure 7). The Cys 27 side chain of CaM is oriented toward the solvent and the bound PLB peptide may not change the environment of the probe, which is why there was less than 10% change in fluorescence intensity. Although there is not a significant change of fluorescence intensity, the synthetic peptide could still be bound to CaM in the N domain while not affecting the environment of the probe.

CaM has a well characterized hydrophobic pocket in the C domain which is involved in binding of CaM receptor peptides and proteins. A mutant chicken CaM (Q143C CaM) which has a cysteine replacing a glutamine at residue 143 in the hydrophobic pocket was produced by Dr. C.L.A. Wang of Boston Biomedical Research Institute. This cysteine residue may be used for site-specific labeling with fluorescent probes. One  $\mu$ M rhodamine-X-maleimide-labeled Q143C CaM was titrated with the synthetic peptide. The change of fluorescence intensity measured at 605 nm was plotted against the concentration of the PLB peptide (Figure 8). The dissociation constant (K<sub>d</sub>) and

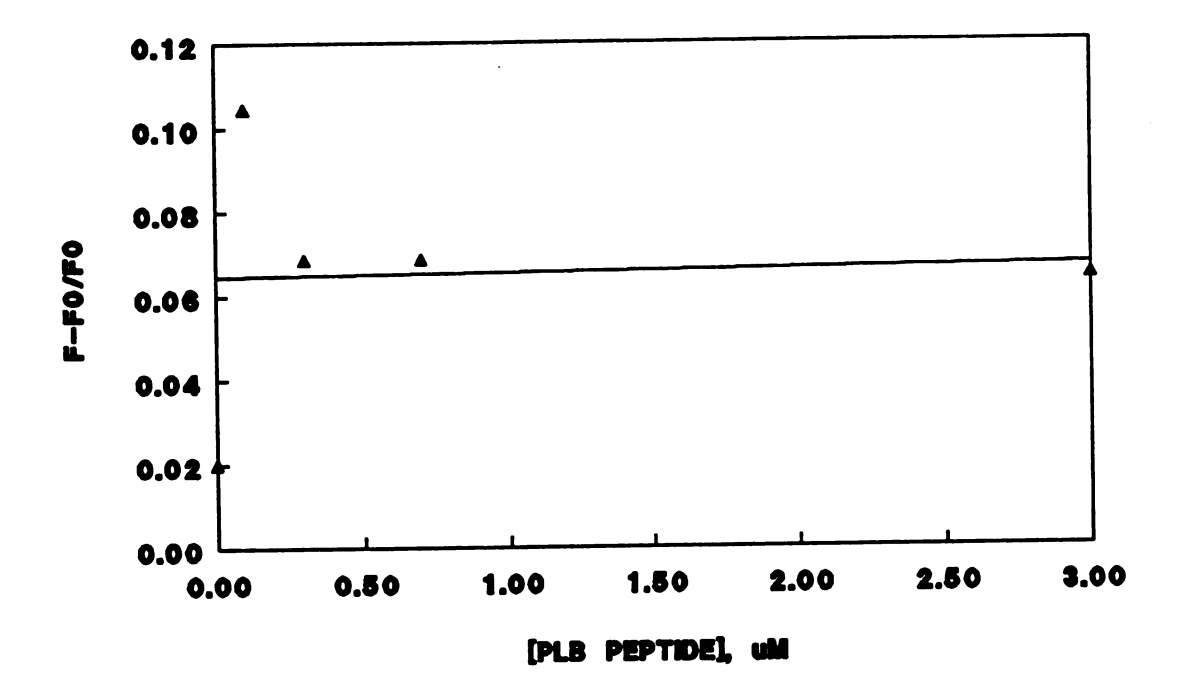


Figure 7. Titration of 1  $\mu$ M rhodamine-X-maleimide labeled wheat germ CaM with PLB peptide (20 mM PIPES, pH 7.5 and 0.1 mM CaCl<sub>2</sub>; excitation wavelength: 580 nm, emission wavelength: 605 nm).

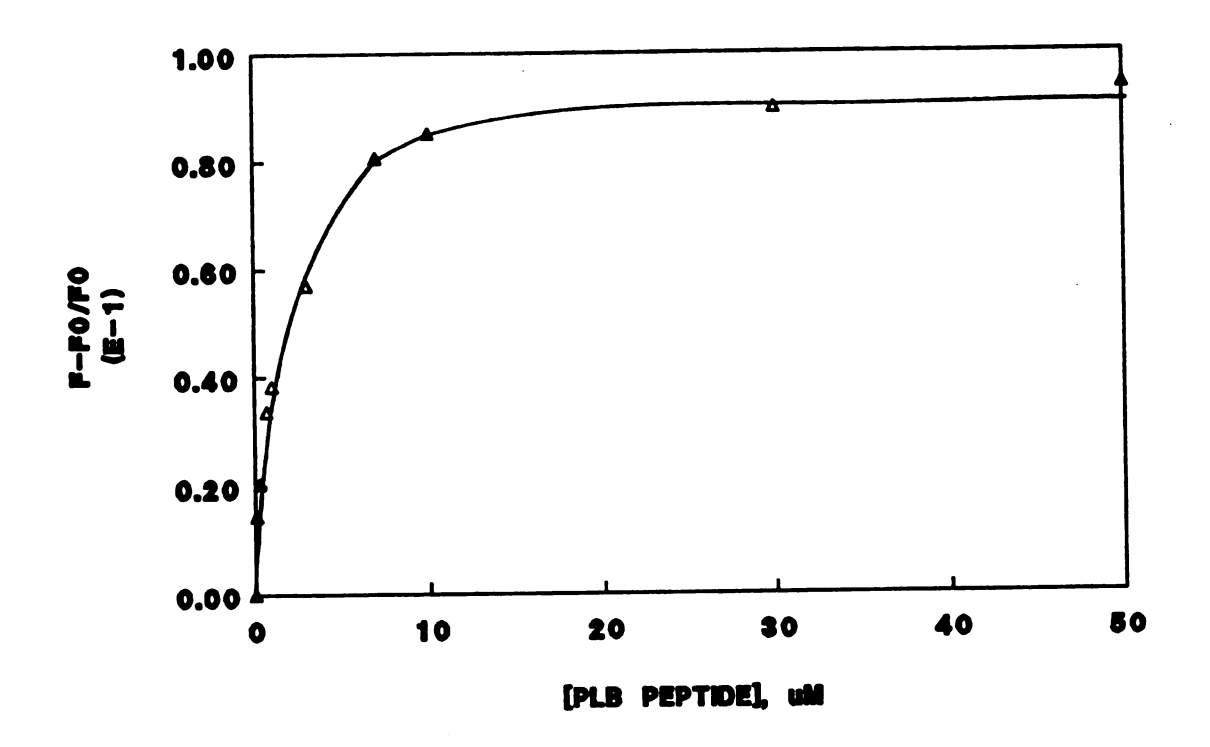


Figure 8. Titration of 1  $\mu$ M rhodamine-X-maleimide labeled site-specific mutant chicken CaM (Q143C CaM) with PLB peptide (20 mM PIPES, pH 7.0, 0.1 M NaCl and 0.1 mM CaCl<sub>2</sub>; excitation wavelength: 580 nm, emission wavelength: 605 nm).

the maximum binding capacity  $(B_{\rm max})$ , calculated from the Scatchard plot (Figure 9), were 1.64  $\mu{\rm M}$  and 1.083 x  $10^{-3}$   $\mu{\rm M}$ , respectively. Figure 10 shows the anisotropy change with incresing peptide concentration. It shows about a 10% increase in the fluorescence anisotropy of rhodamine-labeled CaM upon binding of the PLB peptide. The  $K_{\rm d}$  value was determined as 2.69  $\mu{\rm M}$  from the middle point of titration curve in Figure 11.

In an effort to determine whether the fluorescent probe was affecting the affinity of PLB for CaM and to obtain more precise information on the PLB peptide binding to the CaM, another fluorescence probe, IANBD, was employed in the next study. Compared with rhodamine-X-maleimide (Figure 12), IANBD is a smaller molecule and is generally more sensitive to conformational changes within its environment.

IANBD is small and hydrophobic, and at Cys 143, it is likely embedded in the hydrophobic core of CaM molecule. Upon binding of the PLB peptide to CaM, the fluorescent probe may be pushed out of the hydrophobic pocket of CaM and exposed to solvent. Consequently, absorption of energy of the excited fluorescent probe by the solvent results in a decrease in fluorescence intensity and a red-shift in the spectrum (Figure 13). Coupled with the fluorescence decrease there is a red-shift of 10 nm when the PLB peptide is bound to CaM. The fluorescence intensity of 1  $\mu$ M IANBD-labeled Q143C CaM was measured upon titrating with the synthetic PLB peptide. Figure 14 indicates the fluorescence intensity at 537 nm decreases by 50% as a function of the concentration of added peptide.

<b>₹</b>		
•		
·		

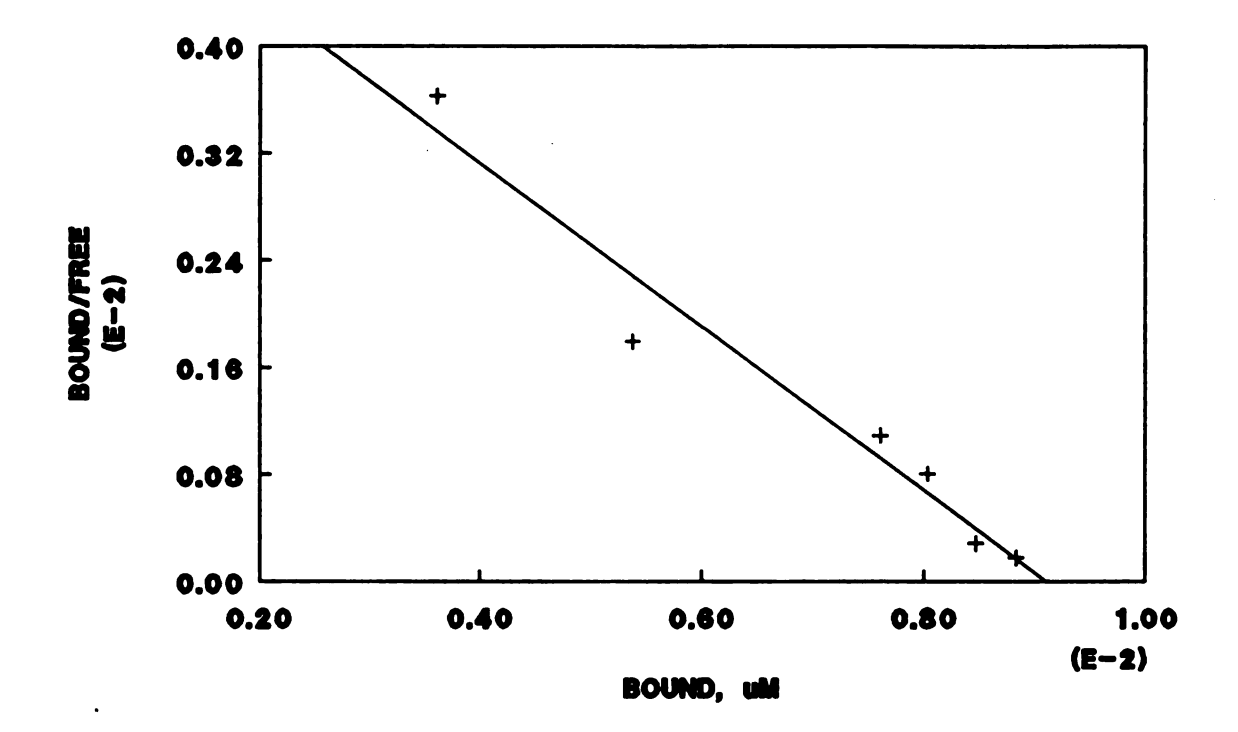


Figure 9. Scatchard plot of rhodamine-X-maleimide-labeled Q143C CaM titration. The value of the dissociation constant ( $K_d$ ) and the maximum binding capacity ( $B_{max}$ ) are 1.64  $\mu$ M and 1.083 x  $10^{-3}$   $\mu$ M, respectively.

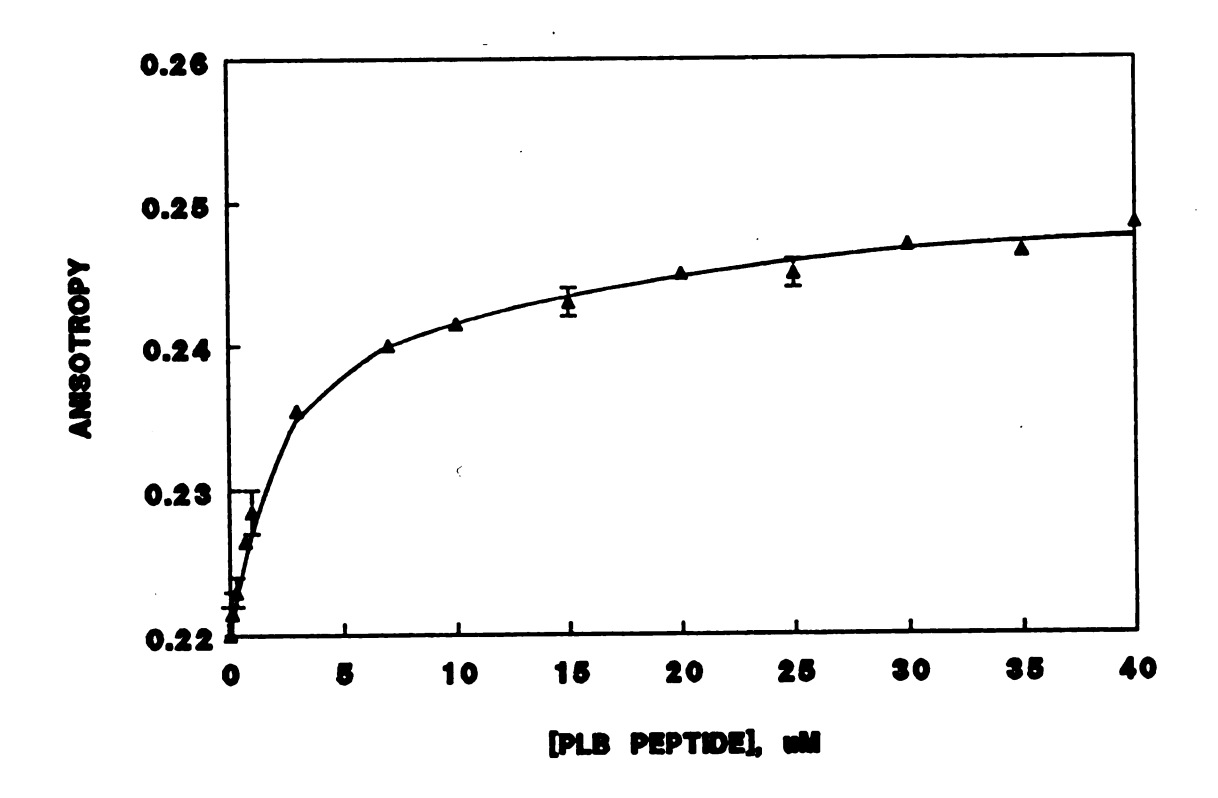


Figure 10. Fluorescence anisotropy measurement upon titration of rhodamine-X-maleimide labeled Q143C CaM with the PLB peptide.

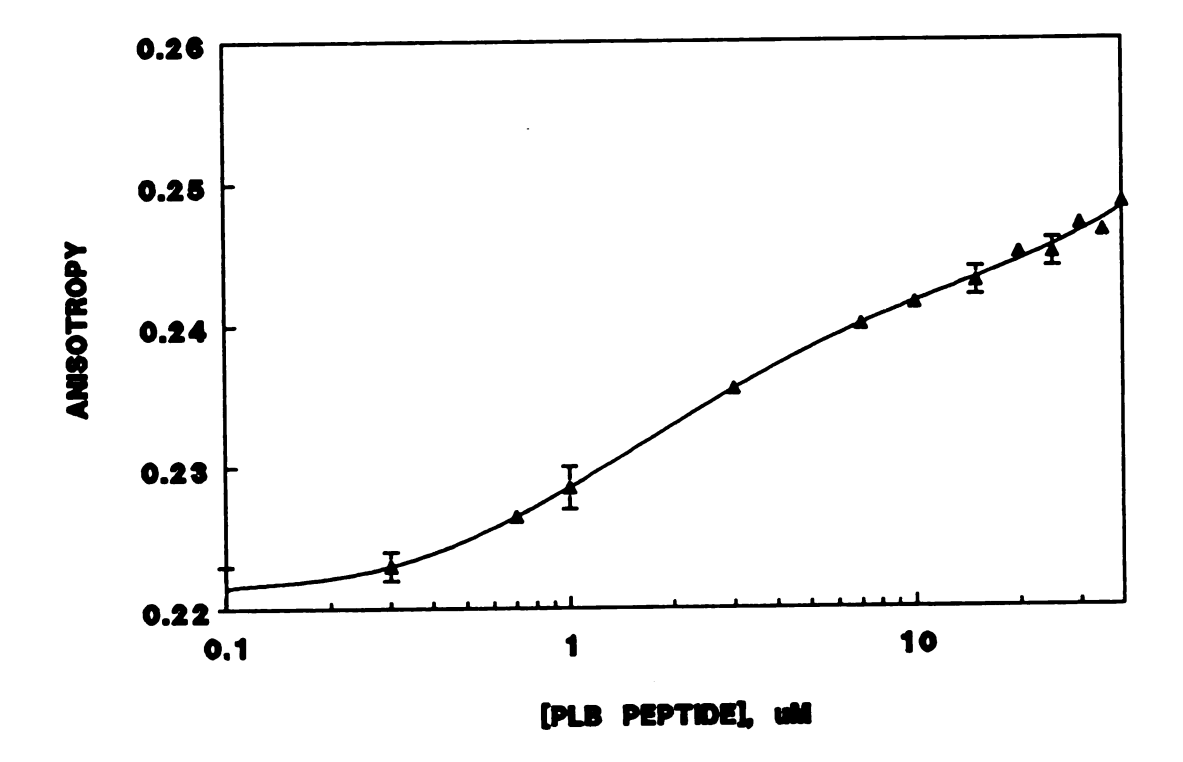


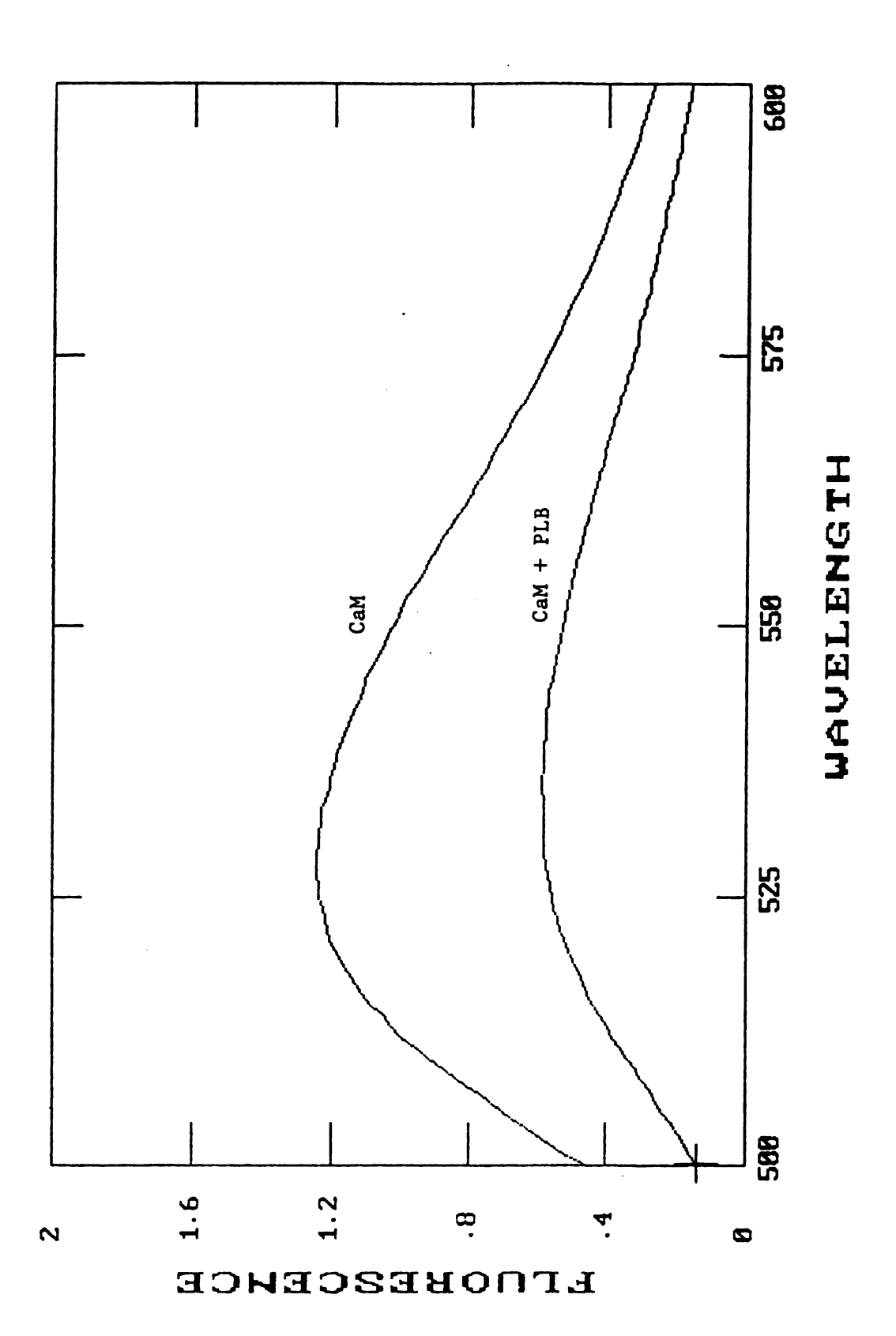
Figure 11. Fluorescence anisotropy change of rhodamine-X-maleimide-labeled Q143C CaM vs concentration of PLB peptide. Kd=2.69  $\mu$ M.

### Rhodamine-X-maleimide

### IANBD

Figure 12. Molecular structures of rhodamine-X-maleimide and N-((2(iodoacetoxy)ethyl-N-methyl)-amino-7-nitrobenz-2-oxa-1,3-diazole) (IANBD).

Figure 13. Fluorescence emission scan of IANBD-labeled Q143C CaM in the presence and absence of the PLB peptide. The excitation wavelength was 475 nm. (20 mM PIPES, pH 7.0, 0.1 M NaCl and 0.1 mM CaCl<sub>2</sub>).



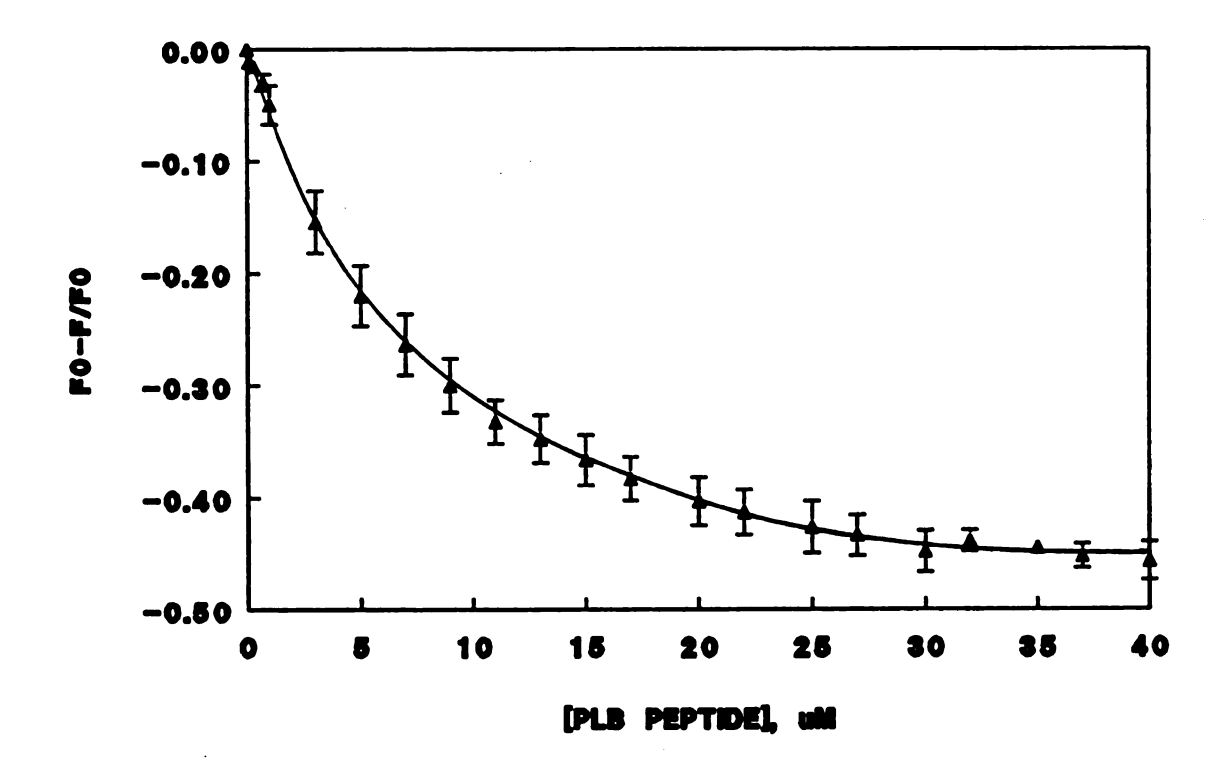


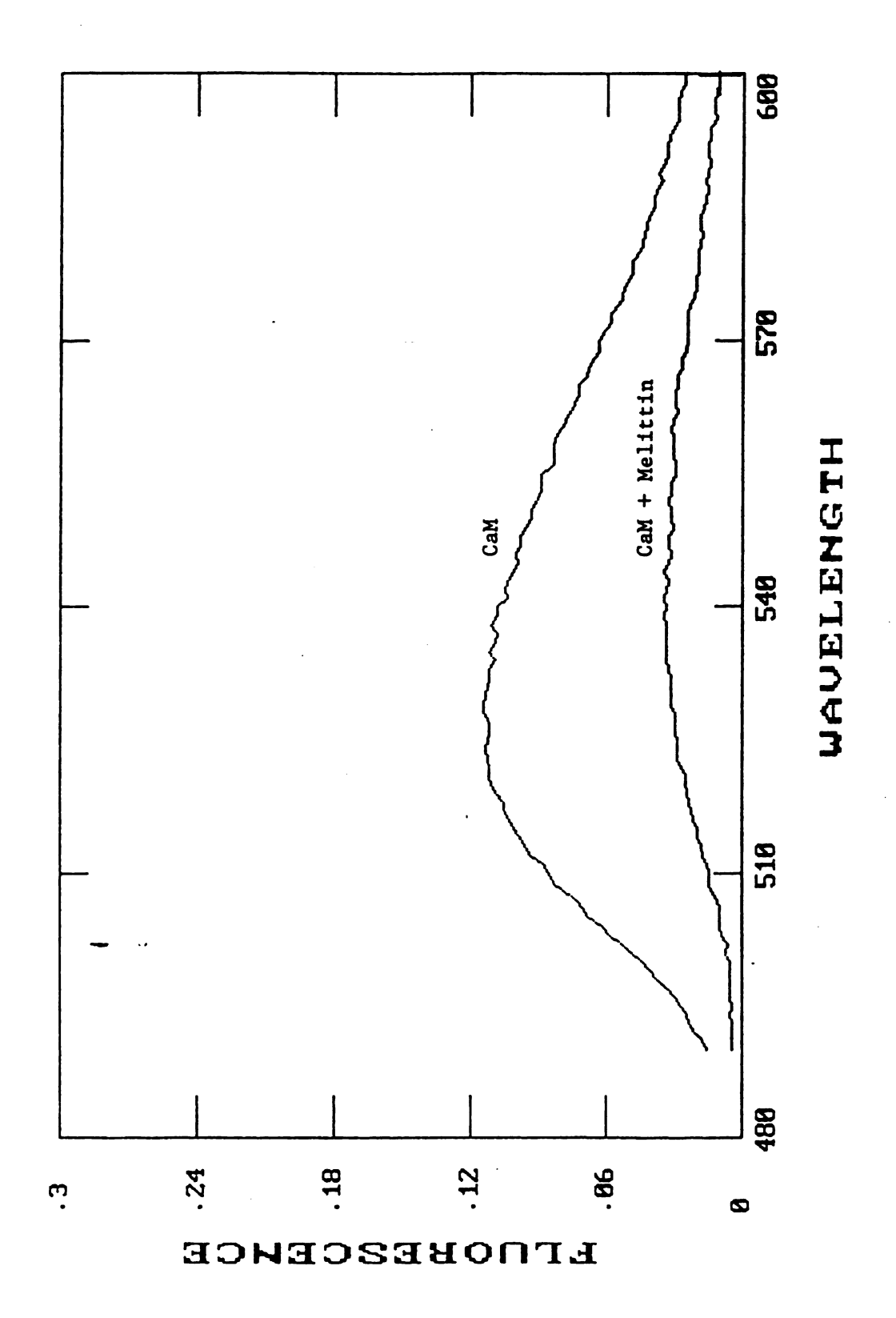
Figure 14. Fluorescence change upon titration of IANBD-labeled Q143C CaM with PLB peptide in 20 mM PIPES, pH 7.0, 0.1 M NaCl and 0.1 mM CaCl<sub>2</sub>. The excitation wavelength was 475 nm; the emission wavelength was 537 nm.

The binding of CaM to the PLB peptide was compared with binding of CaM to melittin, a well characterized CaM-binding peptide (Comte et al., 1983). The fluorescence intensity of IANBD-labeled 0143C CaM at 537 nm decreased with a red-shift of 15 nm upon binding of melittin (Figure 15). Titration of 20 nM IANBD-labeled Q143C CaM with increasing concentration of melittin resulted in about a 60% decrease in fluorescence intensity (Figure 16). It also shows a decrease fluorescence intensity before the concentration of the peptide reaches 40 nM. This indicates that CaM binds to melittin with high affinity and is in agreement with the results of Comte et al.  $(K_d=3 \text{ nM})(1983)$ . Comte's results were verified by Cox and coworkers (1985). Since the fluorescence probe was labeled in the C domain, the fluorescence intensity change suggests that both melittin and PLB bind in the C domain of CaM in the vicinity of Cys 143.

The dissociation constant  $K_d$  for Q143C CaM binding to the PLB peptide, calculated from the Scatchard plot (Figure 17), was 7  $\mu$ M. Meanwhile the maximum binding capacity  $B_{\rm max}$  was determined to be 0.98  $\mu$ M, which indicates that 1 mole of PLB peptide binds 1 mole of CaM.

To determine the affinity of phosphorylated PLB to CaM, the PLB peptide was phosphorylated by cAMP-dependent protein kinase. Then 1  $\mu$ M IANBD-labeled Q143C CaM was titrated with the phosphorylated peptide. The titration curve (Figure 18) shows about a 30% decrease in fluorescence intensity with increasing concentration of the phosphorylated peptide. With

Figure 15. Fluorescence emission spectrum of IANBD-labeled Q143C CaM in the absence and presence of melittin. The excitation wavelength was 475 nm. (20 mM PIPES, pH 7.0, 0.1 M NaCl and 0.1 mM  $CaCl_2$ ).



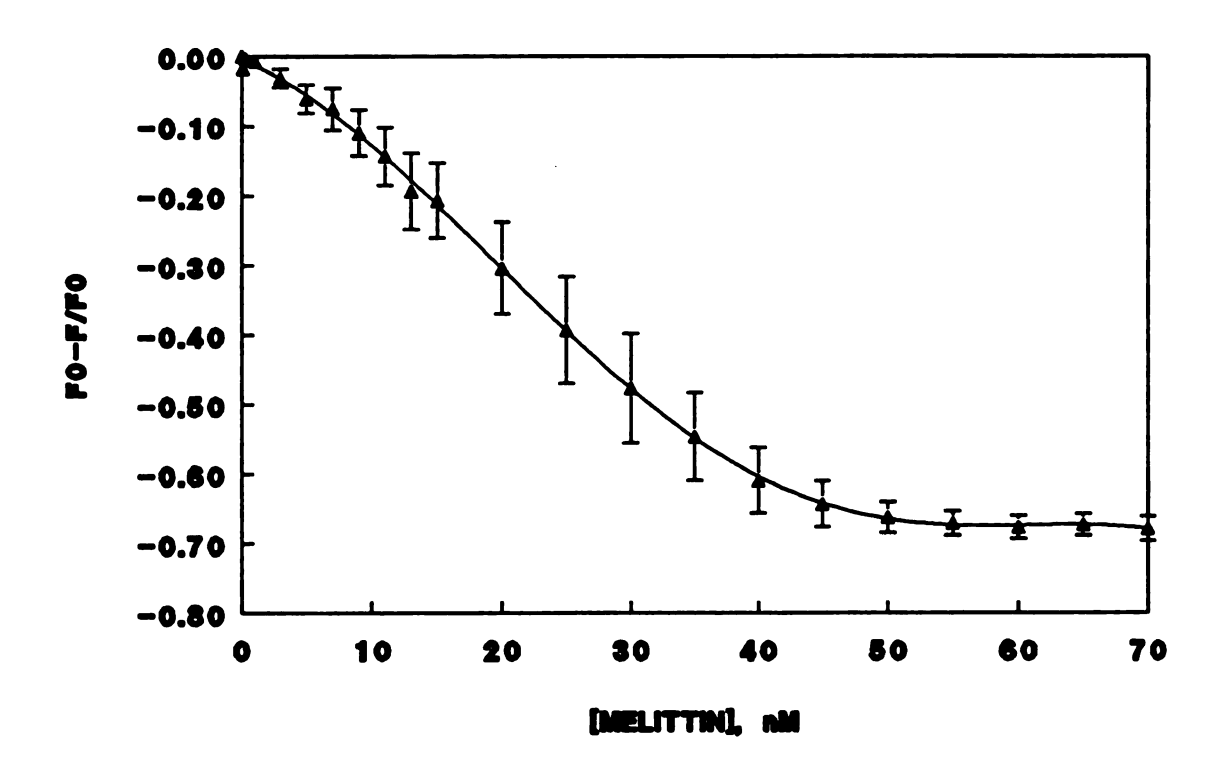


Figure 16. Titration of IANBD-labeled Q143C CaM with melittin. The beffer conditions were 20 mM PIPES, pH 7.0, 0.1 M NaCl and 0.1 mM  $CaCl_2$ . The excitation wavelength was 475nm; the emission wavelength was 537 nm).

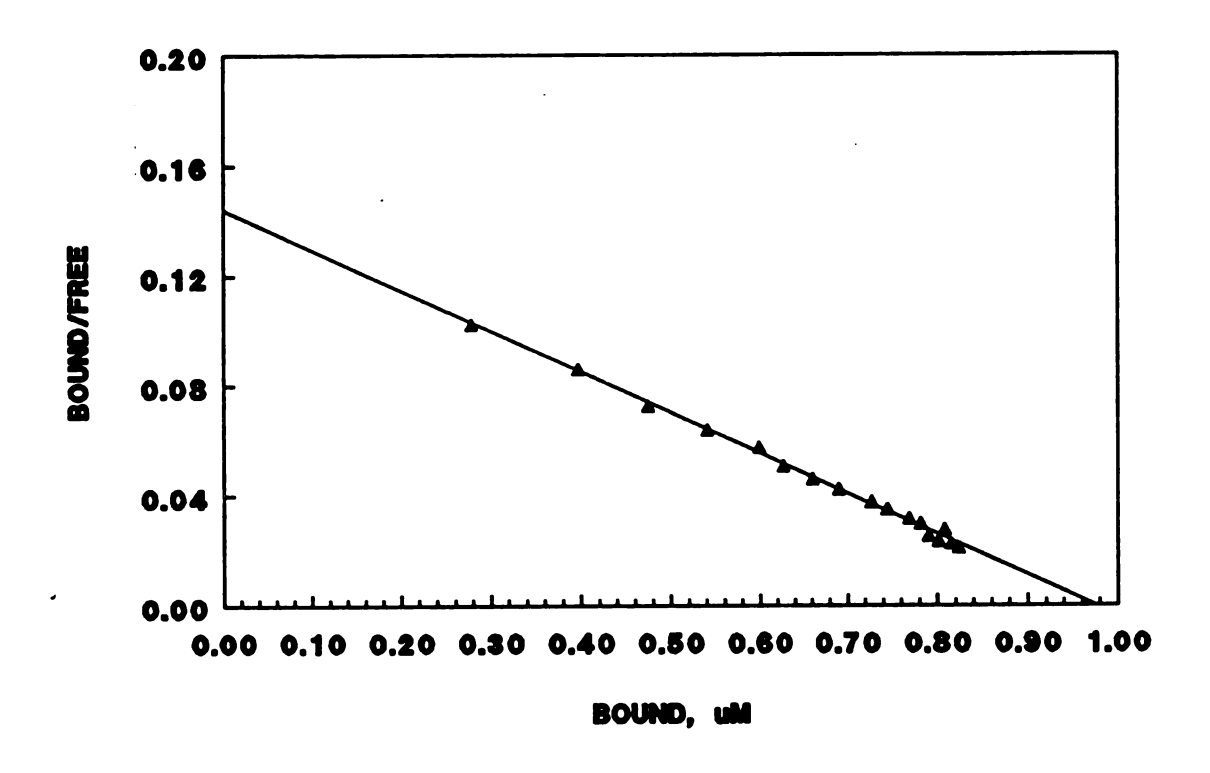


Figure 17. Scatchard plot of titration of IANBD-labeled Q143C CaM with PLB peptide. Kd=7  $\mu\text{M},~B_{\text{max}}\text{=}0.98~\mu\text{M}.$ 

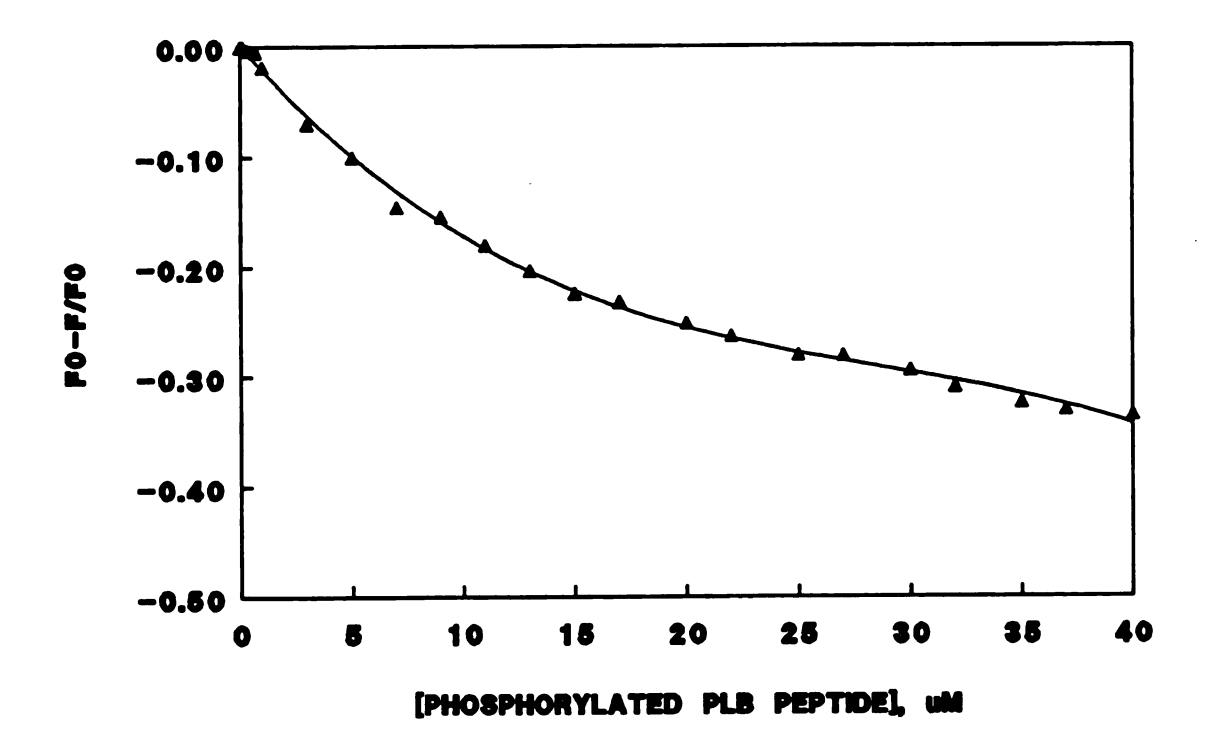


Figure 18. Titration of IANBD-labeled Q143C CaM with cAMP-dependent protein kinase phosphorylated PLB peptide. The buffer conditions were 20 mM PIPES, pH 7.0 and 0.1 mM CaCl<sub>2</sub>. The excitation wavelength was 475 nm; the emission wavelength was 537 nm).

the same analysis methods used for titration of IANBD-labeled Q143C CaM with non-phosphorylated peptide, the Scatchard plot (Figure 19) gives a  $B_{max}$  and  $K_d$  which of 1  $\mu$ M and 17  $\mu$ M, respectively.

Molla et al. (1985) demonstrated that phosphorylation of PLB by either the cAMP-dependent or the CaM-dependent protein kinase results in reduced CaM due to a change in charge of PLB The results obtained in this study show that the cAMP-dependent phosphorylation increases the dissociation constant more than 2-fold (7  $\mu$ M compared with 17  $\mu$ M). On the other hand, the data suggested that CaM and phosphorylated PLB also form a 1:1 complex.

In the contraction-relaxation cycle of cardiac and smooth muscle, phosphorylation of PLB by both cAMP- and CaM-dependent protein kinases can accelerate the relaxation rate by increasing Ca uptake by the SR. Phosphorylated PLB will have a lower affinity to CaM and may no longer be bound to CaM and the CaM-dependent protein kinase dissociates from PLB.

cam target proteins are predicted to be amphiphilic (Cox et al., 1985). Figure 20 shows a helical wheel diagram of a model of amphiphilic peptide [FMOC-(Leu-Lys-Lys-Leu-Leu-Lys-Leu)<sub>2</sub>; LK2], which binds to CaM with affinity as high as that of melittin (Cox et al., 1985). Comparing residues 2-16 of the cytoplasmic portion of PLB with LK2 (Figure 20), residues 2-16 of PLB have fewer hydrophobic residues. Since the density of positive charges on the amphiphilic peptide and the hydrophobic density are two of the factors determining the

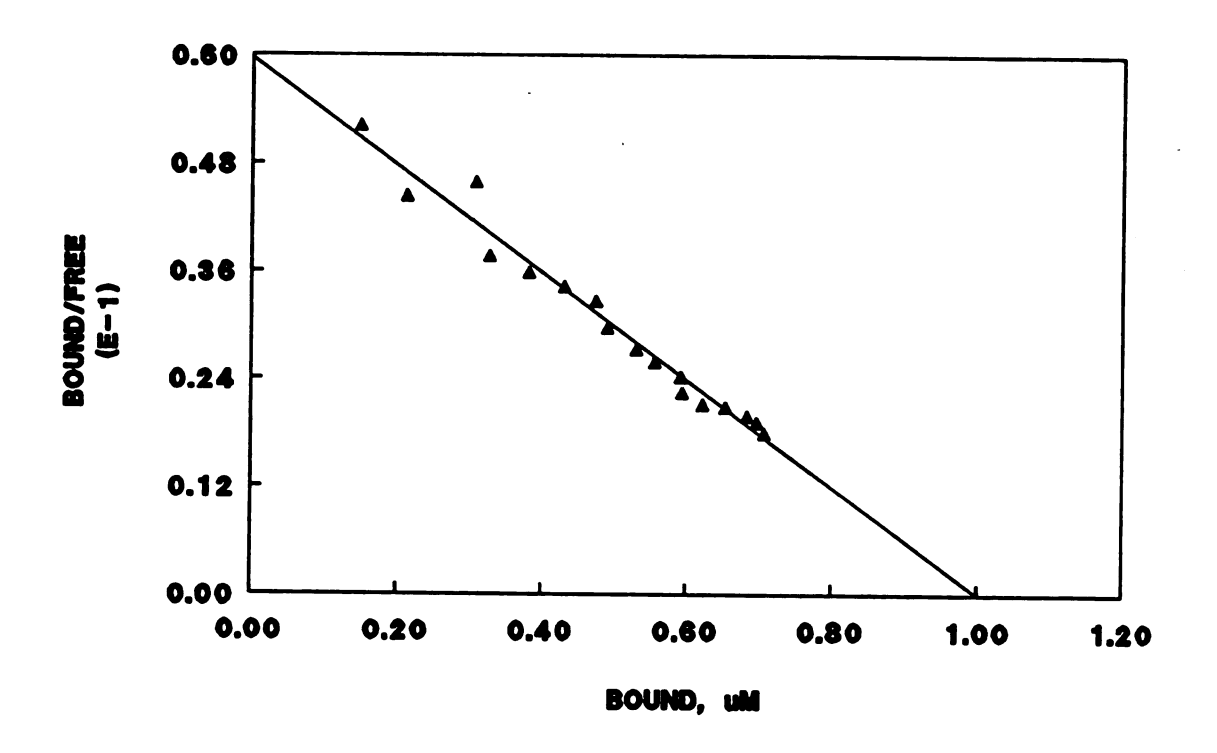


Figure 19. Scatchard plot of titration of IANBD-labeled Q143C CaM with phosphorylated PLB peptide. Kd=16.78  $\mu$ M, B<sub>max</sub>=1  $\mu$ M.

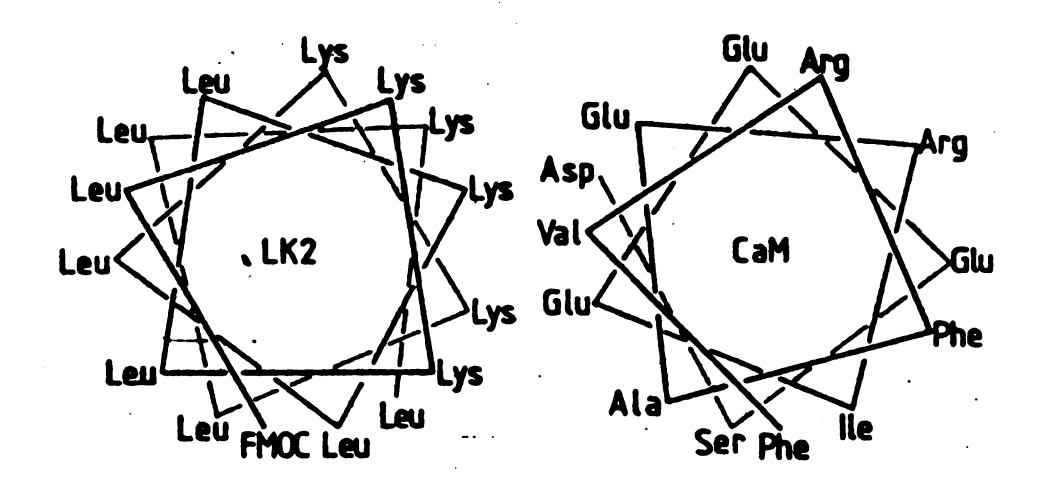


Figure 20. Helical wheel diagram of peptide LK2 (FMOC-(Leu-Lys-Lys-Leu-Leu-Lys-Leu)<sub>2</sub> and phospholamban residues 2-16 (From Cox, Comte, Fitton and DeGrado, 1985, J. Biol. Chem. 260, 2533).

affinity of peptides for CaM binding and it contributes to the stability of the binding (Cox et al., 1985), PLB binds CaM with relatively lower affinity compared with sample peptide LK2 binds CaM.

The crystal structure studies of CaM suggested that the two globular domains of CaM have large, hydrophobic patches which as well as highly negative electrostatic potential for binding positively charged amphiphilic helices (Babu et al., 1985; Kretsinger et al., 1986). Kretsinger (1992) proposed that the entire molecule of CaM may be dumbbell-shaped with the linker connecting the two globular pairs of helix-loophelix Ca<sup>2+</sup> binding domains serving as a flexible-linker. This specific configuration allows peptides such as melittin and proteins, such as muscle light chain kinase (MLCK), which is another well characterized CaM target protein, to bind at both the N- and C-domains of CaM.

While the fluorescence studies neither indicate binding nor non-binding to the N-domain of CaM, NMR studies have suggested that the PLB peptide does bind to the N domain of the CaM (Gao et al., 1992). In these studies, wheat germ CaM was spin-labeled on Cys 27 and titrated with PLB peptide. The observed quenching by the spin-label of specific residues of PLB peptide suggests that the peptide binds to the N-domain of the CaM (Gao et al., 1992). By combining the results of fluorescent and NMR studies, a CaM-PLB binding model is proposed in which PLB binds to both the N- and C-domains of CaM.

There are many forces that may affect the stability of the protein-protein binding, such as van der Waals forces, hydrophobic interactions and electrostatic forces. In this study, the role of electrostatic forces and hydrophobic effects were examed. IANBD-labeled 0143C CaM (with and without PLB peptide) was titrated with increasing concentration of KCl and the fluorescence intensity was monitored as a function of KCl concentration (Figure 21). For the titration of CaM-PLB complex there is an increase in fluorescence intensity, whereas there is a slight decrease in fluorescence intensity for the unbound CaM. The increase in ionic strength upon addition of KCl may result in breaking up the CaM-PLB complex by breaking up the electrostatic interactions between CaM and the PLB peptide. Re-embedded the hydrophobic fluorescence probe into the hydrophobic pocket of CaM results in increasing fluorescent intensity. The sensitivity of this complex to salt concentration suggests that electrostatic interactions play a more significant role than hydrophobic interactions in stabilization of the CaM-PLB complex.

If PLB binds CaM, the functional significance of the role of this interaction must be determined. Hanson et al. (1988) demonstrated that PLB in SR vesicles treated with acchymotrypsin, which most probably resulted in removal of the first 6 residues, was not phosphorylated by CaM-dependent protein kinase and consequently lost the CaM affinity labeling. Phosphorylation by the cAMP-dependent protein kinase, however, remained intact. Their results suggested that

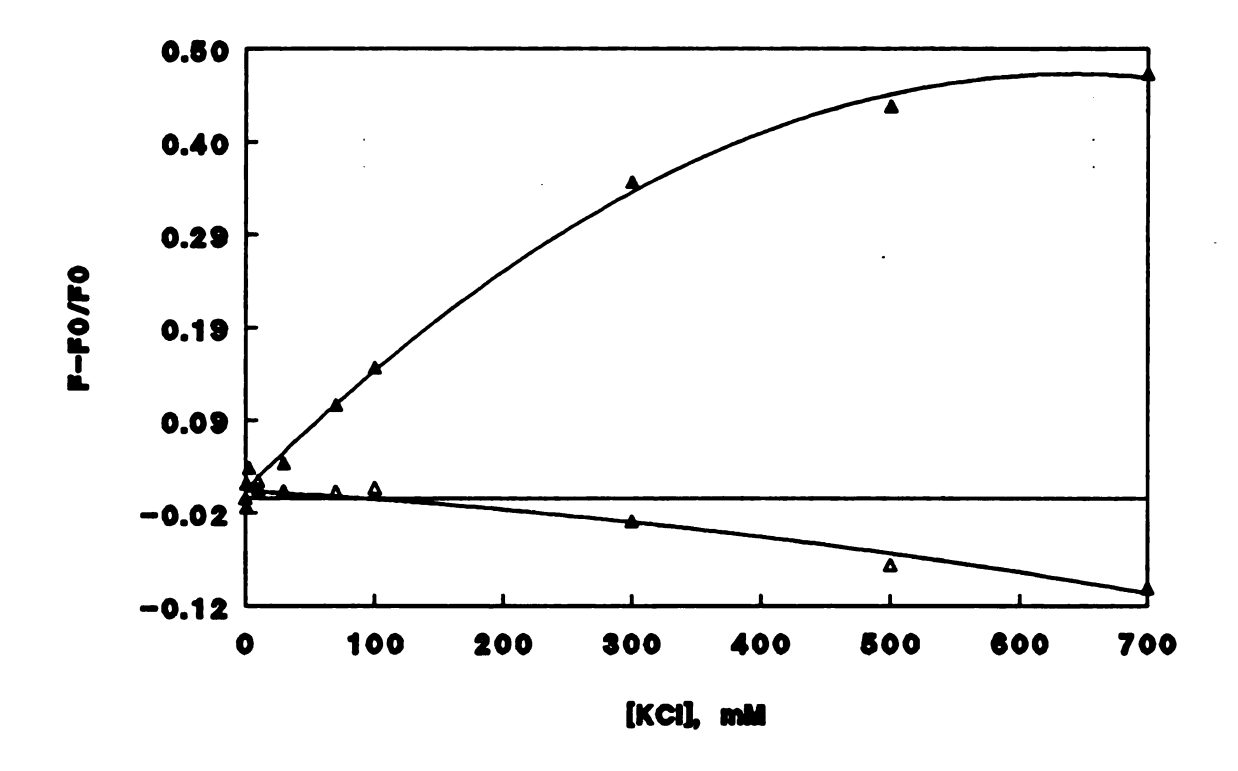


Figure 21. Titration of IANBD-labeled Q143C CaM with KCl in the absence ( $\triangle$ ) or presence ( $\triangle$ ) of 30  $\mu$ M PLB peptide. The buffer condition were 20 mM PIPES, pH 7.0 and 0.1 mM CaCl<sub>2</sub>. The excitation wavelength was 475 nm; the emission wavelength was 537 nm).

the binding of CaM to PLB may be an essential step in the mechanism of CaM-dependent phosphorylation of PLB.

In order to define the site of chymotrypsin cleavage of PLB, the synthetic peptide corresponding to of PLB residues 1-25 (Figure 22) was digested with &-chymotrypsin, an enzyme which preferentially cleaves at aromatic amino acids (Wilcox, 1970). Among the first 25 residues of the synthetic peptide, there is only one aromatic residue, Tyr 6. The digestion products were purified by reverse-phase HPLC and the elution profile (Figure 23) exhibits three peaks. The peptide eluting at 28 minutes was the PLB peptide 1-25 based on co-elution with a standard. Due to lack of absorbance at 280 nm, the peptide eluting at 31 minutes had no tyrosine residue. Sequencing of this fraction indicated that this fraction was composed of residues 7-25. This experiment confirmed that chymotrypsin cleaved at Tyr 6 of PLB.

The third objective of this study is to further investigate the mechanism of CaM-dependent phosphorylation of PLB. To determine whether the first 6 residues bind to CaM for activating CaM-dependent protein kinase, the PLB peptide was digested with varying concentrations of a-chymotrypsin and then phosphorylated by the CaM-dependent protein kinase (Figure 24). The intensity of the bands corresponding to the PLB peptide indicates the extent of phosphorylation. The results clearly shows that phosphorylation decreases with increasing digestion of the peptide by chymotrypsin. <sup>32</sup>P Incorporated into the peptide was determined by scintillation

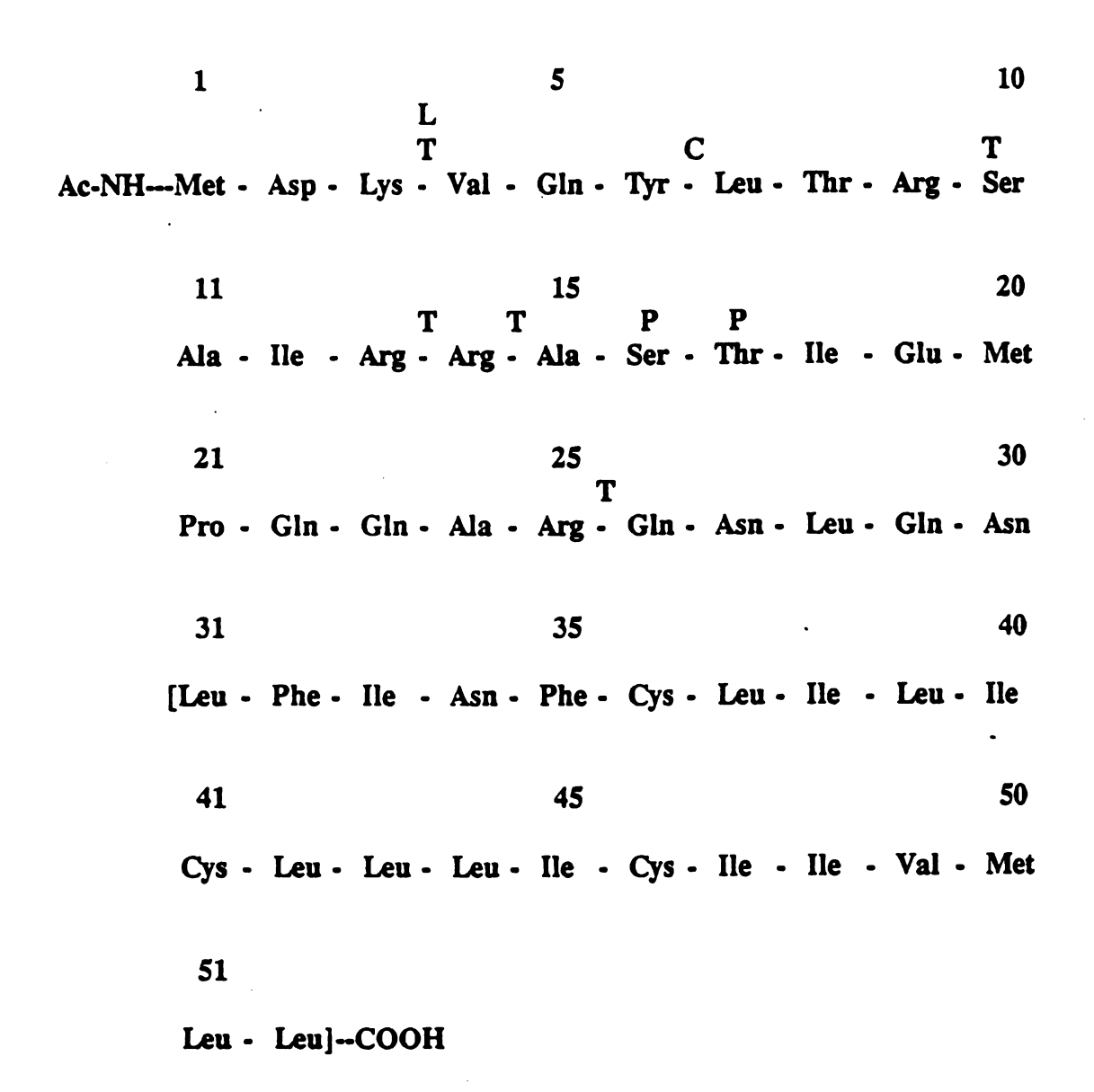


Figure 22. Amino acid sequence of PLB. (From Fujii, Ueno, Kitano, Tanaka, Kadoma and Tada, 1987, J. Clin. Invest. 79, 301-304; Strasburg, Hanson, Ouyang and Louis, 1993, Biochim. Biophys. Acta, In press).

Figure 23. HPLC elution profile of α-chymotrypsin digested PLB peptide. The peptide eluting at 31 minutes was sequenced by Edman degradation and identified as residues 7-25 (From Strasburg, Hanson, Ouyang and Louis, 1993, Biochim. Biophys. Acta, In press).

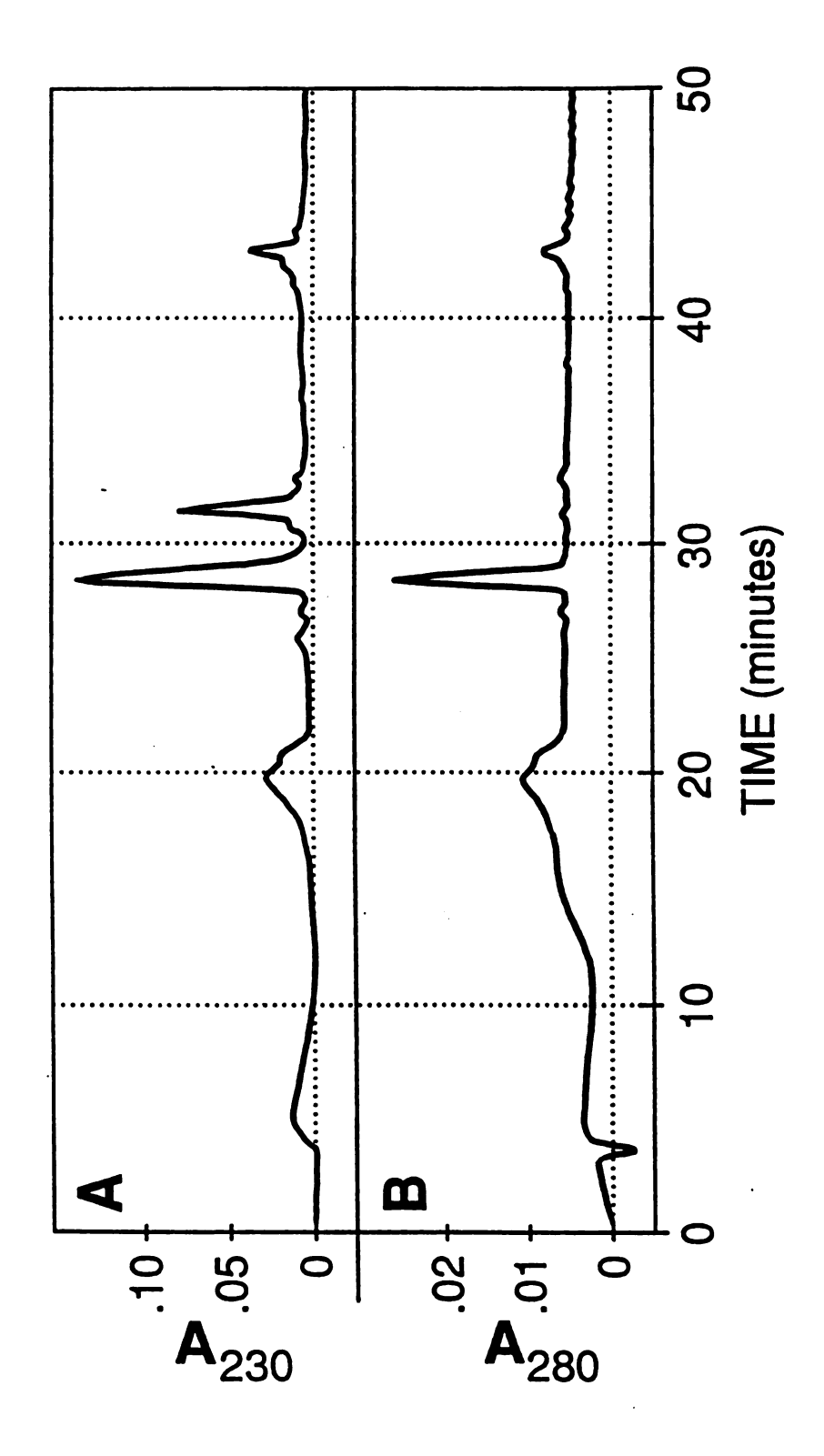
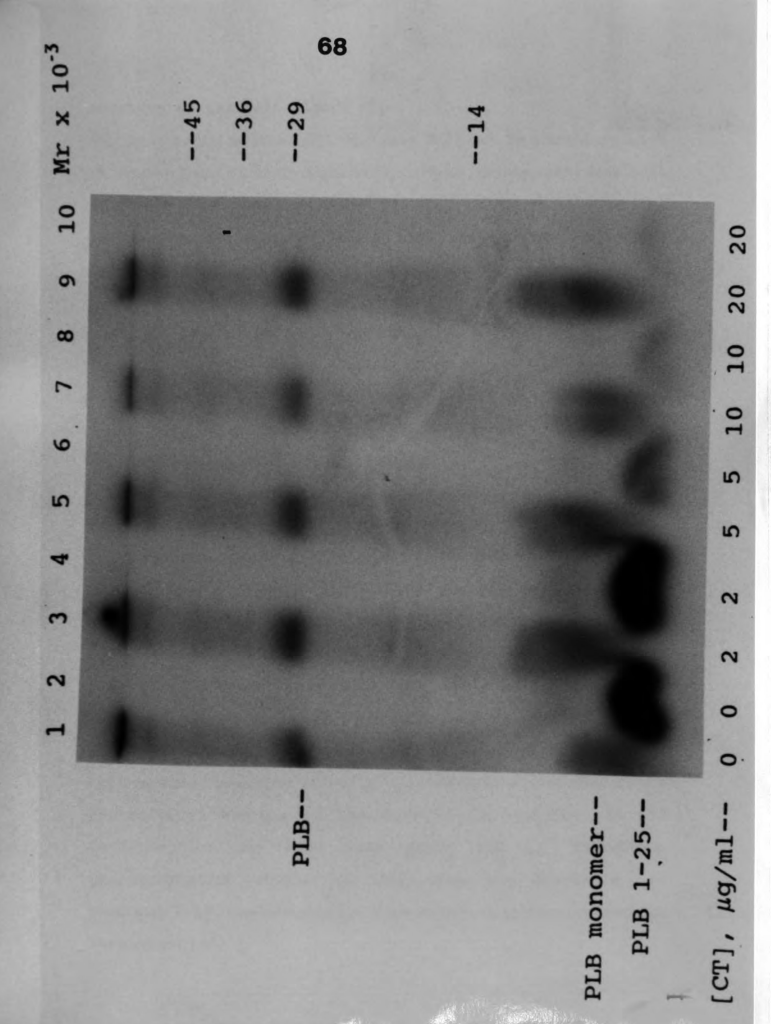


Figure 24. Autoradiogram of phosphorylation of  $\alpha$ -chymotrypsin digested PLB peptide by CaM-dependent protein kinase. 5  $\mu$ g of digested PLB peptide were phosphorylated in 20 mM HEPES, pH 6.8, 0.1 mM CaCl<sub>2</sub>, 10 mM MgCl<sub>2</sub>, 1  $\mu$ M wheat germ CaM, 1 mg/ml longitudinal SR vesicles and 0.1 mM AT<sup>32</sup>P. The gel was exposed for 24 hours. The concentrations of  $\alpha$ -chymotrypsin are: Lane 1: 0  $\mu$ g/ml, Lane 2: 2  $\mu$ g/ml, Lane 3: 5  $\mu$ g/ml, Lane 4: 10  $\mu$ g/ml, Lane 5, 20  $\mu$ g/ml. Odd and even numbered lanes represent SR membrane and supernatants which contain phosphorylated PLB peptide, respectively.



	/ 1		
			1
			1
			1
			i

counting of the gel (Figure 25).

To confirm whether PLB residues 7-25 can be phosphorylated by either CaM- or cAMP-dependent protein kinase, residues 7-25 of PLB peptide were purified by HPLC. This portion of the peptide has the phosphorylation sites for both CaM- and cAMP-dependent protein kinases, Thr 17 and Ser 16, respectively. As was observed with the chymotryptic treatment of SR vesicles, CaM-dependent phosphorylation of the PLB peptide did not occur (Figure 26). This result indicates that even though the PLB peptide 7-25 has the phosphorylation site for CaM-dependent protein kinase as in the SR vesicles, it is not phosphorylated by the CaM-dependent protein kinase.

To exam the ability of the cAMP-dependent protein kinase to phosphorylate the purified PLB peptide 7-25, the peptide was incubated under conditions for phosphorylation by this kinase. Inspite the presence of the phosphorylation site on this peptide, it was not phosphorylated. This unexpected result may be caused by a conformational change of the peptide following the proteolysis which makes the phosphorylation site inside of the molecule. It is also possible that the K<sub>N</sub> value, which is defined as the substrate concentration that gives half-maximal reaction velocity, is reduced as a result of the proteolysis, whereas in the case of SR vesicles the PLB concentration may have been above the K<sub>N</sub>. Therefore; phosphorylation occurs by increasing the substrate, or residues 7-25, concentration. This aspect will require further investigation.

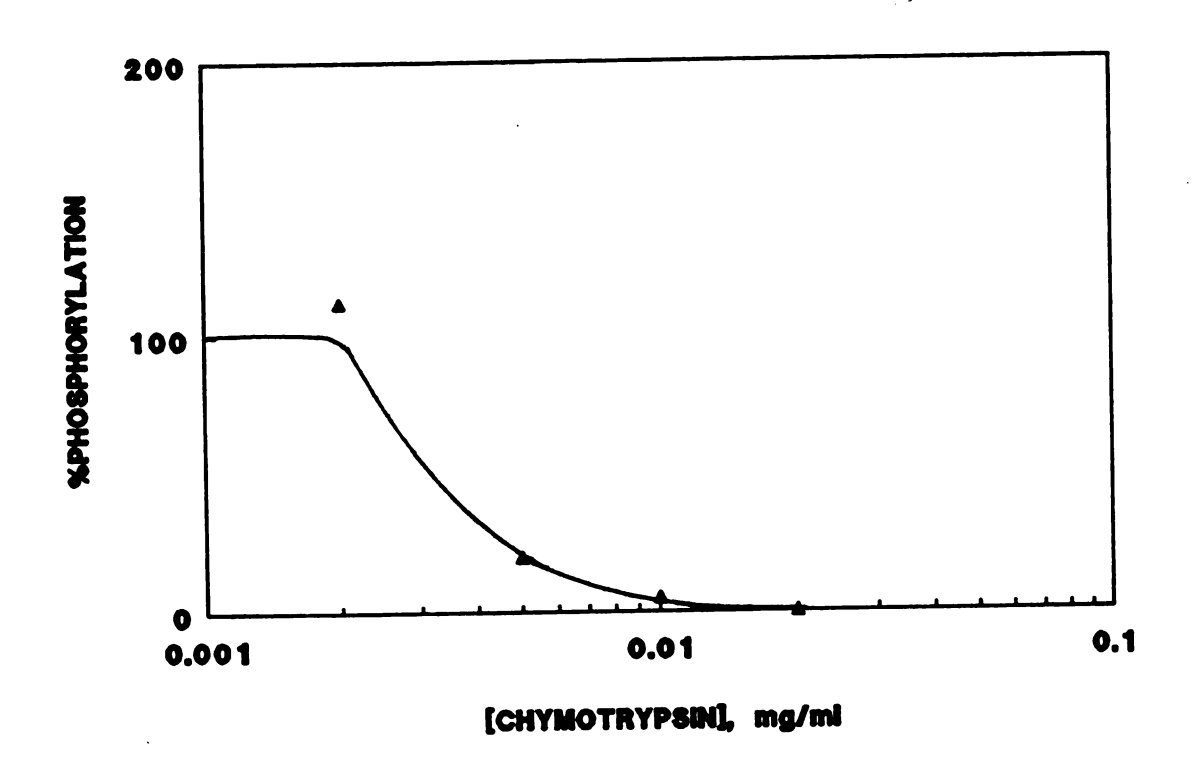
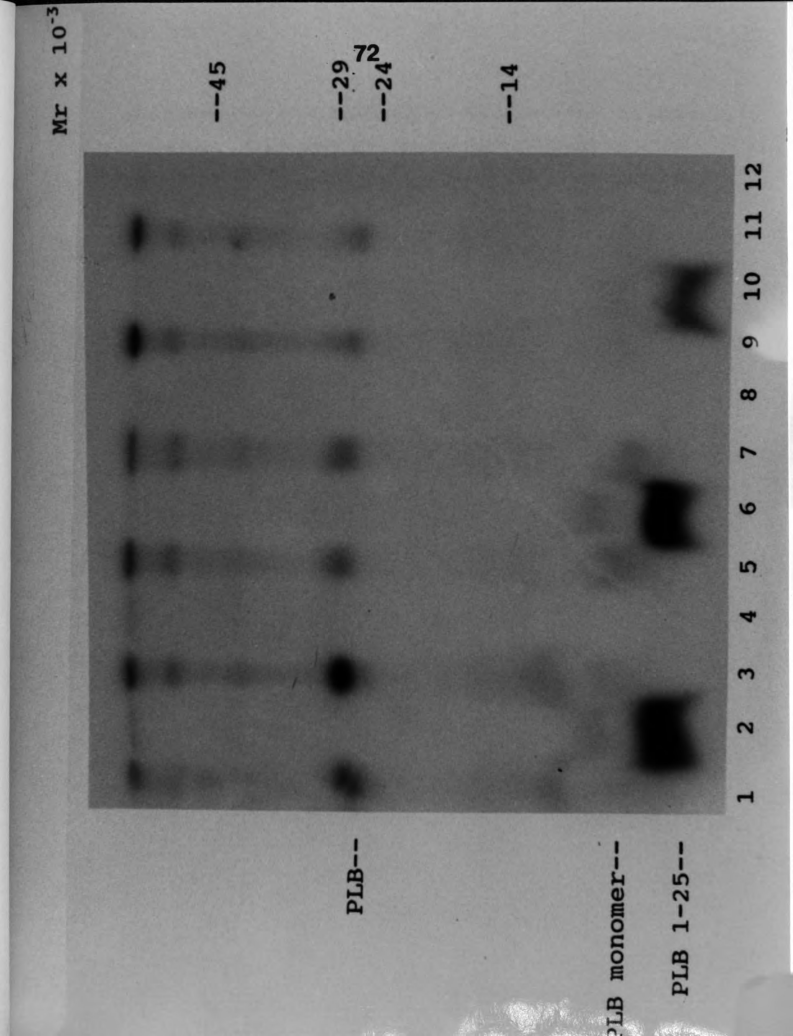


Figure 25. Percentage of phosphorylations of chymotrypsin-digested PLB peptide as a function of chymotrypsin concentration.

Figure 26. Autoradiogram of phosphorylation of PLB peptide 1-25 and 7-25 by CaM- and cAMP-dependent protein kinase. Five μq of the peptides were phosphorylated in 20 mM HEPES, pH 6.8, 10 mM MgCl2, 2 mM EGTA, 10 mM cAMP, 0.25 mg/ml protein kinase and 0.1 mM AT32P for cAMP-dependent phosphorylation. For CaMdependent phosphorylation, 5 µg of peptide were phosphorylated in 20 mM HEPES, pH 6.8, 0.1 mM CaCl<sub>2</sub>, 10 mM MgCl<sub>2</sub>, 1  $\mu$ M wheat germ CaM, 1 mg/ml longitudinal SR vesicles and 0.1 mM AT32P. The peptides were separated from the SR membrane and resolved in a 20% polyacrylamide gel, and the gel was dried and was exposed for 24 hours. The reaction conditions for the control were 20 mM HEPES, pH 6.8, 2 mM EGTA 5  $\mu$ g PLB petides and 1 mM AT<sup>32</sup>P. Lane 1 and 2, 5 and 6, and 9 and 10: PLB peptide 1-25, Lane 3 and 4, 7 and 8, 11 and 12: PLB peptide 7-25. Lane 1 to 4: cAMP-dependent phosphorylation, Lane 5 and 8: CaM-dependent phosphorylation, Lane 11 and 12: Control. Odd and even numbered lanes represent SR membrane and supernatants. phosphorylation,



The proteolytic studies support the hypothesis that CaM binds to the first 6 residues of PLB, and that formation of a CaM-PLB complex is an important mechanism for activating CaM-dependent phosphorylation of PLB by CaM-dependent protein kinase.

## CONCLUSION

The results of this study demonstrate that the synthetic peptide corresponding PLB 1-25 residues binds to the C-domain of CaM with a stoichiometry 1:1 and a dissociation constant  $(K_d)$  of 7  $\mu$ M. Phosphorylation of PLB peptide by cAMP-dependent protein kinase decreases its affinity to CaM ( $K_d=16.8 \mu M$ ). The ionic strength study suggests that the electrostatic forces rather than hydrophobic forces are a major force involved in stabilizing the CaM-PLB complex. Removal of the first 6 residues of the PLB peptide 1-25 prevented phosphorylation by CaM-dependent protein kinase. This observation suggests that binding of the first 6 residues of PLB to CaM is significant for activating CaM-dependent protein kinase to phosphorylate PLB peptide 7-25. PLB peptide which does not have first 6 residues cannot be phosphorylated by cAMP-dependent protein kinase either due to decreasing the K value or conformational change of the peptide.

## LITERATURE CITED

Babu, Y.S., Sack, J.S., Greenhough, T.J., Bugg, C.E. Means, A.R. and Cook, W.J. 1985, Three-dimensional structure of calmodulin. Science 315, 37-39.

Bastide, F., Meissner, G., Fleischer, S. and Post, R. 1973. Similarity of the active site of phosphorylation of the adenosine triphosphatase for transport of sodium and potassium ions in kidney to that for transport of calcium ions in the sarcoplasmic reticulum of muscle. J. Biol. Chem. 248, 8385-8391.

Bendall, J.R. 1952. Effect of the 'Marsh factor' on the shortening of muscle fibre models in the presence of adenosine triphosphate. Nature 170, 1058-1060.

Bendall, J. R. 1958. Muscle-relaxing factors. Nature 181, 1188-1190.

Bennett, H.S. and Porter, K.R. 1953. An electron microscope study of sectioned breast muscle of the domestic fowl. Am. J. Anat. 93, 61-105.

Blumenthal, D.K., Takio, K., Edelman, A.M., Charbonneau, H. Titani, K., Walsh, K.A. and Krebs, E.G. 1985. Identification of the calmodulin-binding domain of skeletal muscle myosin light chain kinase. Proc. Natl. Acad. Sci. U.S.A. 82, 3187-3191.

Bozler, E. 1954. Binding of calcium and magnesium by the contractile elements. J. Gen. Physiol. 38, 735-742.

Carsten, M.E. 1964. The cardiac calcium pump. Proc. Natl. Acad. Sci. USA 52, 1456-1462.

Cheung, W.Y. 1980. Calmodulin plays a pivotal role in cellular regulation. Science 207, 19-27.

Comte, M., Maulet, Y., and Cox, J.A. 1983. Ca<sup>2+</sup>-dependent high-affinity complex formation between calmodulin and melittin. Biochem. J. 209, 289-302.

Cox, J.A., Comte, M., Fitton, J.E. and DeGrado, W.F. 1985. The interaction of calmodulin with amphiphilic peptides. J. Biol. Chem. 260, 2527-2534.

Degani, C. and Boyer, P.D. 1973. A borohydride reduction

method for characterization of the acyl phosphate linkage in proteins and its application to sarcoplasmic reticulum adenosine triphosphatase. J. Biol. Chem. 23, 8222-8226.

De Meis, L. and Vianna, A.L. 1979. Energy interconversion by the Ca<sup>2+</sup>-dependent ATPase of the sarcoplasmic reticulum. Ann. Rev. Biochem. 48, 275-292.

Ebashi, S. 1960. Calcium binding and relaxation in the actomyosin. J. Biochem. 48, 150-151.

Ebashi, S. 1961. Calcium binding activity of vesicular relaxing factor. J. Biochem. 50, 236-244.

Ebashi, S. and Ebashi, F. 1962. Removal of calcium and relaxation in actomyosin systems. Nature 194, 378-379.

Ebashi, S. and Endo, M. 1968. Ca ion and muscle contraction. Progr. Biophys. Mol. Biol. 18, 123-183.

Elberton, N.R. and Isenberg, I. 1969. Fluorescence polarization study of DNA-proflavine complexes. Biopolymers 8, 767-786.

Endo, M. 1964. Entry of a dye into the sarcotubular system of muscle. Nature 202, 1115-1116.

Fawcett, D.W. and McNutt, N.S. 1969. The ultrastructure of the cat myocardium. J.Cell Biol. 42, 1-45.

Franzini-Armstrong, C., Landmesser, L. and Pilar, G. 1975. Size and shape of transverse tubule openings in frog twitch muscle fibers. J. Cell. Biol. 64, 493-497.

Fujii, J., Ueno, A., Kitano, K., Tanaka, S., Kadoma, M. and Tada, M. 1987. Complete complementary DNA-derived amino acid sequence of canine cardiac phospholamban. J. Clin. Invest. 79, 301-304.

Gao, Y., Levine, B.A., Mornet, D. Slatter, D.A. and Strasburg, G.M. 1992. Interaction of calmodulin with phospholamban and caldesmon: comparative studies by 'H-NMR spectroscopy. Biochim. Biophys. Acta 22-34.

Guilbault, G.G. 1973. Practical Fluorescence: Theory, Methods, and Techniques. Marcel Dekker, Inc. New York.

Hanson, T., Strasburg, G. and Louis, C.F. 1988. Characterization of the region phospholamban that interact with calmodulin. Biophys. J. 53:M-Pos188.

Harigaya, S. and Schwartz, A. 1969. Rate of calcium binding and uptake in normal animal and failing human cardiac muscle.

Membrane vesicles (relaxing system) and mitochondria. Circulation Res. 25, 781-794.

Hasselbach, W. and Makinose, M. 1961. Die Calciumpumpe der "Erschlaffungsgrana" des Muskels und ihre Abbängigkeit von der ATP-Splaltung. Biochem. Z. 333, 518-528.

Hasselbach, W. and Makinose, M. 1963. Über den Mechanismus des Calciumtransportes durch die Membrane des sarkoplasmatischen Reticulums. Biochem. Z. 339, 94-111.

Heilbrunn, L.V. and Wiercinski, F.J. 1947. The action of various cations on muscle protoplasm. J. Cellular Comp. Physiol. 29, 15-32.

Huxley, H.E. 1964. Evidence for continuity between the central elements of the triads and extracellular space in frog sartorius muscle. Nature 202, 1067-1071.

Ikemoto, N., Bhatnagar, G.M. and Gergely, J. 1971. Fractionation of solubilized sarcoplasmic reticulum. Biochem. Biophys. Res. Commun. 44, 1510-1517.

Ikura, M., Clore, G.M., Gronenborn, A.M., Zhu, G., Klee, C.B. and Bax, A. 1992. Solution structure of a calmodulin-target peptide complex by multidimensional NMR. Science 256, 632-638.

Inesi, G. 1972. Active transport of calcium ion in sarcoplasmic membranes. Ann. Rev. Biophys. Bioeng. 1, 191-210.

James, P., Inui, M., Tada, M. Chiesi, M. and Carafoli, E. 1989. Nature and site of phospholamban regulation of the Ca<sup>2+</sup> pump of sarcoplasmic reticulum. Nature 342, 90-92.

Jones, L.R., Simmerman, H.K.B., Gurd, F.R. and Wegener, A.D. 1985. Purification and characterization of phospholamban from canine cardiac sarcoplasmic reticulum. J. Biol. Chem. 260, 7721-7730.

Kamada, T. and Kinoshita, H. 1943. Disturbances inhibited from naked surface of muscle protoplasm. Japan. J. Zool. 10, 469-493.

Katz, S. and Repke, D.I. 1967. Quantitative aspects of dog cardiac microsomal calcium binding and calcium uptake. Circulation Res. 21, 153-162.

Katz, S. and Retulla, M.A. 1978. Phosphodiesterase protein activator stimulates calcium transport in cardiac microsomal preparation enriched in sarcoplasmic reticulum. Biochem. Biophys. Res. Commun. 1373-1379.

Katz, A.M. 1979. Role of the contractile proteins and sarcoplasmic reticulum in the response of the heart to catecholamines: An historical review. Adv. Cyclic Nucleotide Res. 332-341.

Kirchberger, M.A., Tada, M. And Katz, A.M. 1974. Adenosine 3':5'-monophosphate-dependent protein kinase-catalyzed phosphorylation reaction and its relationship to calcium transport in cardiac sarcoplasmic reticulum. J. Biol. Chem. 249, 6166-6173.

Klee, C.B., Crouch, R.H. and Richman, P.G. 1980. Calmodulin. Ann. Rev, Biochem. 49, 489-515.

Klee, C.B. and Vanaman, T.C. 1982. Calmodulin. Adv. Protein Chem. 35, 213-321.

Kretsinger, R.H. 1976. Calcium-binding proteins. Ann. Rev. Biochem. 45, 239-266.

Kretsinger, R.H. 1980. Structure and evolution calcium-modulation protein. CRC Crit. Rev. Biochem. 8, 119-174.

Kretsinger, R.H., Rudnick, S.E. and Weissman, L.J. 1986. Crystal structure of calmodulin. J. Inorg. Biochem. 289-302.

Kretsinger, R.H. 1992. Calmodulin and myosin light chain kinase: how helices are bent. Science 258, 50-51.

Kugami, H., Ebashi, S. and Takeda, F. 1955. Essential relaxing factor in muscle other than myokinase and creatine phosphokinase. Nature 176, 166.

Laemmli, U.K. 1970. Cleavage of structural protein during the assembly of the head of bacteriophage T. Nature, 227, 680-685.

Lakowicz, J.R. 1983. Principles of Fluorescence spectroscopy. New York: Plenum Press.

LaRaia, P.J. and Morkin, E. 1974. Adenosine 3':5'-monophosphate-dependent membrane phosphorylation. A possible mechanism for the control of microsomal calcium transport in heart muscle. Circulation Res. 35, 298-306.

Le Peuch, C.J., Haiech, J. and Demaille, J.G. 1979. Concerted regulation of cardiac sarcoplasmic reticulum calcium transport by cyclic adenosine monophosphate dependent and calcium-calmodulin-dependent phosphorylation. Biochemistry 18,5150-5157.

Le Peuch, C.J., Le Peuch, D.A.M., and Demaille, J.G. 1980. Phospholamban activator of the cardiac sarcoplasmic reticulum calcium pump. Physicochemical properties and diagonal

purification. Biochemistry 19, 3368-3373.

Levison, S.A. 1975. Fluorescence polarization kinetic studies of macromolecular reactions. Biochemical Fluorescence Concepts. Chen, R.F. and Edelhoch, H. (ed.) Marcel Dekker, New York. 1, 375-408.

Lopashuk, P. Richter, B. and Katz, S. 1980. Characterization of calmodulin effects on calcium transport in cardiac microsomes enriched in sarcoplasmic reticulum. Biochemistry 19, 5603-5607.

Louis, C.F. and Maffitt, M. 1982. Characterization of calcium-mediated phosphorylation of cardiac muscle sarcoplasmic reticulum. Arch. Biochem. Biophys. 218, 109-118.

Louis, C.F. and Jarvis, B. 1982. Affinity labeling of calmodulin-binding components in canine cardiac sarcoplasmic reticulum. J. Biol. Chem. 257, 15187-15191.

Lowry, O.H., Rosebrough, N.J., Farr, A.L. and Randall, R.J. 1951. Protein measurement with Folin phenol reagent. J. Biol. Chem. 193, 265-275.

Lukas, T.J., Burgess, W.H., Prendergast, F.G., Lau, W. and Waltterson, D.M. 1986. Calmodulin binding domains: Characterization of a phosphorylation and calmodulin binding site from myosin light chain kinase. Biochemistry 25, 1458-1464.

MacLennan, D.H. and Holland, P.C. 1975. Calcium transport in sarcoplasmic reticulum. Ann. Rev. Biophys. Bioeng. 4, 377-404.

MacLennan, D.H., Brandl, C.J., Korczak, B. and Green, N.M. 1985. Amino-acid sequence of a Ca2+ + Mg2+-dependent ATPase from rabbit muscle sarcoplasmic reticulum, deduced from its complementary DNA sequence. Nature 316, 696-700.

Marsh, B.B. 1951. A factor modifying muscle fibre synaeresis. Nature 167, 1065-1066.

Martonosi, A. and Halpin, R.A. 1971. Sarcoplasmic reticulum X. The protein composition of sarcoplasmic reticulum membrane. Arch. Biochem. Biophys. 144, 66-77.

Means, A.R., VanBerkum, M.F.A., Bagchi, I., Lu, K.P. and Rasmussen, C.D. 1991. Regulatory functions of calmodulin. Pharmac. Ther. 50, 255-270.

Meissner, G. 1973. ATP and Ca<sup>2+</sup> binding by the Ca<sup>2+</sup> pump protein of sarcoplasmic reticulum. Biochim. Biophys. Acta 298, 906-926.

Molla, A., Capony, J.P. and Demaille, J.G. 1985. Cardiac sarcoplasmic-reticulum calmodulin-binding protein. Biochem. J. 226, 859-865.

Muscatello, U.E. Anderson-Cedergren, E., Azzone, G.F. and von der Decken, A. 1961. The sarcotubular system of frog skeletal muscle. A morphophological and biochemical study. J. Biophys. Biochem. Cytol. Suppl. 10, 201-218.

Muscatello, U.E. Anderson-Cedergren, E. and Azzone, G.F. 1962. The mechanism of muscle-fiber relaxation. Adenosine triphosphatase and relaxing activity of the sarcotubular system. Biochim. Biophys. Acta 63, 55-74.

Nagai, T., Makinose, M. and Hasselbach, W. 1960. Der physiologische Erschlaffungsfaktor und die Muskelgrana. Biochim. Biophys. Acta 43, 223-238.

Nilsson, J., von Euler, A.M. and Dalsgard, C.J. 1985. Stimulation of connective tissue cell growth by substance P and substance K. Nature 315, 61-63.

O'Neil, K.T., Wolfe, H.R., Jr. Erickson-Viltanen, S. and DeGrado, W.F. 1987. Fluorescence properties of calmodulin-binding peptides reflect alpha-helical periodicity. Science 236, 1454-1456.

O'Neil, K.T., and Degrado, W.F. 1990. How calmodulin binds its targets: sequence independent recognition of amphiphilic  $\alpha$ -helices. Trends Biochem. Sci. 15, 59-64.

Peachey, L.D. 1965. The sarcoplasmic reticulum and transverse tubules of the frog's sartorius. J. Cell Biol. 25, 209-231.

Peachey, L.D. and Schild, R.F. 1968. The distribution of the T-System along the sarcommeres of frog and toad sartorius muscles. J. Physiol., London 194, 249-258.

Porter, K.R. and Palade, G.E. 1957. Studies on the endoplasmic reticulum. III. Its form and distribution in stiated muscle cells. J. Biophys. Cytol. 3, 269-299.

Porter, K.R. 1961. The sarcoplasmic reticulum. Its recent history and present status. J. Biophys. Biochem. Cytol. Suppl. 10, 219-226.

Shigekawa, M., Finegan, J.M. and Katz, A.M. 1976. Calcium transport ATPase of canine cardiac sarcoplasmic reticulum. J. Biol. Chem. 251, 6894-6900.

Shigekawa, M. and Dougherty, J.P. 1978. Reaction mechanism of Ca<sup>2+</sup>-dependent ATP hydrolysis by skeletal muscle sarcoplasmic reticulum in the absence of added alkali metal salts. J. Biol.

- Chem. 253, 1451-1457.
- Simmermnan, H.K., Collins, J.H., Theibert, J.L. Wegener, A.D. and Jones, L.R. 1986. Sequence analysis of phospholamban. J. Biol. Chem. 261, 13333-13341.
- Simmerman, H.K., Lovelace, D.E. and Jones, L.R. 1989. Secondary structure of detergent-solubilized phospholamban, a phosphorylatable, oligomeric protein of cardiac sarcoplasmic reticulum. Biochim. Biophys. Acta 997, 322-329.
- Smith, P.K., Krohn, R.I., Hermanson, G.T., Mallia, A.K., Gartner, F.H., Provenzano, M.D., Fujimoto, E.K., Goeke, N.M., Olson, B.J. and Klenk, D.C. 1985. Measurement of protein using bicinchoninic acid. Anal. Biochem. 150, 76-85.
- Strasburg, G.M. Hogen, M. Birmachu, W. Thomas, D.D. and Louis, C.F. 1988. Site-specific derivatives of wheat germ calmodulin. J. Biol. Chem. 263, 542-548.
- Strasburg, G.M., Hanson, T.P., Ouyang, H.X. and Louis, C.F. 1993. Localization and functional role of the calmodulin binding domain of phospholamban in cardiac sarcoplasmic reticulum vesicles. Biochim. Biophys. Acta (In press).
- Suko, J., Vogel, H.K. and Chidsey, C.A. 1970. Intracellular calcium and myocardial contractility. Circulation Res. 27, 235-247.
- Suko, J. 1973. The calcium pump of cardiac sarcoplasmic reticulum. Functional alterations at different levels of thyroid state in rabbits. J. Physiol., London 238, 563-582.
- Tada, M., Kirchberger, M.A., Repke, D.I. and Katz, A.M. 1974. The stimulation of calcium transport in cardiac sarcoplasmic reticulum by adenosine 3':5'-monophosphate-dependent protein kinase. J. Biol. Chem. 249, 6174-6180.
- Tada, M., Kirchberger, M.A.and Katz, A.M. 1975. Phosphorylation of a 22,000-dalton component of the cardiac sarcoplasmic reticulum by adenosine 3':5'-monophosphate-dependent protein kinase. J. Biol. Chem. 250, 2640-2647.
- Tada, M., Yamamoto, T. and Tonomura, Y. 1978. Molecular mechanism of active calcium transport by sarcoplasmic reticulum. Physiol. Rev. 58, 1-79.
- Tada, M., Ohmori, F., Yamada, M. and Abe, H. 1979. Mechanism of the stimulation of Ca<sup>2+</sup>-dependent ATPase of cardiac sarcoplasmic reticulum by adenosine 3':5'-monophosphate-dependent protein kinase. J. Biol. Chem. 254, 319-326.
- Tada, M., Yamada, M., Ohmori, F., Kuzuya, T., Inui, M. and

- Abe, H. 1980. Transient state kinetic studies of Ca<sup>2+</sup>-dependent ATPase and calcium transport by cardiac sarcoplasmic reticulum. J. Biol. Chem. 255, 1985-1992.
- Tada, M. and Katz, A.M. 1982. Phosphorylation of the sarcoplasmic reticulum and sarcolemma. Ann. Rev. Physiol. 44, 401-423.
- Tada, M. and Inui, M. 1983. Regulation of calcium transport by the ATPase-phospholamban system. J. Mol. Cell. Cardiol. 15, 565-575.
- Tada, M., Shigekawa, M. and Nimura, Y. 1984. Uptake of calcium by the sarcoplasmic reticulum and its regulation and functional consequences. Physiology and Pathophysiology of the Heart (N. Sperelakis, ed), 255-277. Nijhoff, The Hague.
- Tada, M., Kadoma, M. Inui, M. and Fuji, J. 1988. Regulation of Ca<sup>2+</sup>-pump from cardiac sarcoplasmic reticulum. Methods in Enzymology 157, 107-154.
- Visser, A.J.W.G. and Lee, J. 1980. Lumazine protein from the bioluminescent bacterium *Photobacterium phosphoreum*. A fluorescence study of the protein-ligand equilibrium. Biochemistry 19, 4366-4372.
- Watanabe, S. 1955. Relaxing effects of EDTA on glycerol-treated muscle fibers. Arch. Biochem. Biophys. 54, 559-562.
- Watanabe, S. and Sleator, JR, W. 1957. EDTA relaxation of glycerol-treated muscle fibers, and the effect of magnesium, calcium and manganese ions. Arch. Biochem. Biophys. 68, 81-101.
- Weber, A. 1961. Regulatory mechanisms of the calcium transport system of fragmented sarcoplasmic reticulum. II. Inhibition of outflux in calcium-free media. J. Gen. Physiol. 57, 64-70.
- Weber, A. and Herz, R. 1963. The binding of calcium to actomysin systems in relation to their biological activity. J. Biol. Chem. 238, 599-605.
- Wegener, A.D. and Jones, J.R. 1984. Phosphorylation-induced mobility shift in phospholamban in sodium dodecyl sulfate-polyacrylamide gels. J. Biol. Chem. 259, 1834-1841.
- Wilcox, P.E. 1970. Chymotrypsinogens-chymotrypsins. Methods in Enzymology. Academic Press, New York. 19, 41-64.
- Yamada, S. and Tonomura, Y. 1972. Phosphorylation of the Ca<sup>2+</sup>-Mg<sup>2+</sup>-dependent ATPase of the sarcoplasmic reticulum coupled with cation translocation. J. Biochem. 71, 1101-1104.

Yoshida, M,, Minowa, O. and Yagi, K. 1983. Divalent cation binding to wheat germ calmodulin. J. Biochemistry (Tokyo) 94, 1925-1933.

